Universitat
de les Illes Balears

Title: Forecast sensitivity analysis of the November 7th 2014 medicane

AUTHOR: Aina Maimó Far

Master's Thesis

Master's degree in Advanced Physics and Applied Mathematics
(With a speciality/Itinerary Geophysical Fluids)
at the

UNIVERSITAT DE LES ILLES BALEARS

Academic year: 2017-2018

Date: 22 June 2018

UIB Master's Thesis Supervisor: Víctor Homar Santaner

Contents

1 Introduction

1.1 Predictability. Prediction error. Social impacts

A prediction is a description of the future state of a system. In general, a prediction depends on the entire system state, whether all of it is being predicted or only one of its variables. For the case of hydrometeorological phenomena, their predictions depend on the full states of both the atmosphere and the land surface. Meteorological predictions are as old as human kind. They started as basic estimations of future weather aspects based on experience and have reached a high level of complexity and refinement over the years. The first scientific weather forecasts begun in the 1860's in the UK, led by the pioneering meteorologist vice admiral Robert FitzRoy. Not only did he introduce weather forecasting as we know it today, but he also ended up establishing a meteorological service in the UK that would later become the current MetOffice.

Forecasting the atmosphere is highly valuable for several reasons. A first reason, which is the one motivating this master's thesis, is the scientific challenge it represents and the intellectual value associated with the understanding of the atmospheric system that surrounds us. A second reason, and the most important for the whole of society, is the economic impact associated with weather phenomena and its linked decision making. On the one hand, agriculture and farming depend highly on the atmospheric state. Other highly sensitive industries to the atmospheric state are construction, energy and transportation sectors. On the other hand, there is a strong human societal factor, embedding civil protection in general and particularly risk management as a very important business component of insurance companies. Another reason as to why weather forecasting is important, the least important to society as a whole but the most important to each of its individuals, is the way it affects each person in its daily life. This "group" of reasons includes the answers to such questions as "should I take an umbrella today?" or "is it going to rain during my football game this weekend?". This type of decisions are not usually life or death, but they certainly have large effects in the lives of the people they concern. Amazingly, any improvements in weather prediction ought to seamlessly benefit macroeconomic figures as well as the everyday life of citizens.

If predicting the state of the atmosphere is so crucial to so many factors, it seems strange that weather forecasts still have so much to improve. This is due to the existence of a predictability limit. The predictability of something is the property it has of being predictable, in other words, whether it is possible to know its future state and how much of it. Jule Gregory Charney, one of the most important figures in the history of numerical weather prediction, already stated in 1951 that "the atmosphere exhibits no periodicities of the kind that enable one to predict the weather in the same way one predicts the tides" (Charney, 1951). The person that has made the most fundamental statement on predictability to date is Edward Norton Lorentz, who during the 1960s concluded that "even with perfect models and virtually perfect observations, the chaotic nature of the atmosphere would impose a finite limit of about two weeks to the predictability of the weather" (Lorenz, 1963). He elaborated this theory after running a simple model and then running it again, accidentally introducing really small perturbations in the initial conditions. This tiny difference was amplified with the evolution of time and after a couple of weeks these two states were not distinguishable from two random states of the model. Lorentz's discovery started the theory of chaos, which was later an important factor to the operational introduction of ensemble forecasting systems.

When talking about predictability, it is important to notice that it depends on the scales, both temporal and spatial which need to be consistent with one another. It is way beyond the predictable limit to estimate temperature at a certain point to the hundredth of a degree in two years' time. Similarly, forecasting the mean temperature over a large area in the next minute has a doubtful, if

any, value, so the balance between spatial and temporal precision of predictions is crucial. Many definitions of the predictability limit are possible, but the factors that determine it are always the same: system dynamics and the presence of inevitable errors. System dynamics present an intrinsic limit to the predictability. Errors limit the predictability of the system both technically and in an intrinsic way. Technical errors can be (and are being) reduced as years pass by means of technical and strategic improvements to the observing systems. However, intrinsic errors, specially representativeness errors remain a problem which can not be solved by a mere increase in precision and will most likely be a challenge for years to come.

1.2 The Medicane of November 7, 2014

The Mediterranean is located in mid latitudes and is characterized by the presence of typically baroclinic extratropical cyclones. However, recent studies raised attention to a special type of cyclone with tropical features. These tropical-like cyclones are called Medicanes (from a combination of the words *Mediterranean* and *hurricane*). They generate over the sea, deepen as a result of intense latent heat release and interactions with the sea surface, and lose most of their power when they make landfall. When Medicanes reach populated coastlands, the impacts on people and economic assets are frequently severe. Beyond the scientific challenge of fully understanding their lifecycle, this possibility of severe losses is what makes Medicanes a necessary subject of study, since their potential damages are devastating.

The first step towards a Medicane-ready society is to improve our understanding of their physical properties and prediction limits. With this in mind, several studies have been conducted in order to understand the main processes that drive their formation (e.g. Miglietta et al, 2013). The most identifiable feature of Medicanes comes from satellite imagery, where they can be seen as organized cloud systems spinning cyclonically around a cloudless eye. The main form to identify them in meteorological maps is from the isolated sea level pressure low and the warm core over low-level temperature maps. However, these are necessary but not sufficient conditions to identify a cyclonic system as a Medicane. Further properties need to be present in order to characterize a concrete episode as a Medicane. The problem lies in the fact that these properties require an understading of the physical processes involved in the cyclone formation and this can not usually be done instantly at the time of the event. Medicanes still need further investigation and are a subject of active research (Mazza et al, 2017; Romero and Emanuel, 2017; Cioni et al, 2016).

From what is currently known, and differently from common tropical cyclones, Medicanes are favored by the presence of an upper level trough (Tous and Romero, 2013). This synergizes with the surface low and helps intensify the cyclone. However, the most defining feature is the tropical-like processes that take place inside the cyclone. The relatively warm sea surface temperature is accompanied by intense evaporation. The air parcels near the sea get warmer than the environment and ascend, nearly saturated. When they get above the lifting condensation level, the formation of water droplets by condensation begins, releasing latent heat in the process and further enhancing the cloud development, and also making the center of the cyclone warmer than its surroundings. This release of latent heat is an important process in the deepening of the cyclone and is crucial to its identification as a Medicane (Carrió et al, 2017).

Despite these known general characteristics, some challenges about Medicane formation and evolution still remain. A deeper understanding of the physical processes driving their initiation and evolution would help clarify how they are created and predict whether they will form or not.

Also, the knowledge of how they behave in their environments can give further information on the cyclone tracks, a key component in the prediction of their destructive power and specially of the areas they will affect. There is still a very low predictability associated to these cyclones, caused by their formation over the sea, where observations are scarce, and so analysis errors are an important limiting factor.

The Medicane studied in this work took place during the 7^{th} of November but its causes and effects covered the days from the 5^{th} to the 8^{th} of November. During the 5^{th} and the 6^{th} of November a prominent ridge progressing over the north Atlantic coincided with an intense trough moving towards the Mediterranean. Despite these already present cyclonic conditions, it wasn't until the 7^{th} of November when a small intense cyclone formed. It developed its strongest phase near the coasts of Malta and Tunisia, also affecting the Italian islands of Sicily and Lampedusa. After its strongest phase, it evolved and moved towards the north-east, reaching Sicily and initiating the decaying phase. The cyclone is clearly detected in both satellite images and conventional weather stations observations. Satellite imagery showed a cloudless eye surrounded by a dense cloud structure (figure 1a) whereas the meteorological station in Malta detected a pressure drop exceeding 20hPa in 6 hours (figure 1b), accompanied by wind gusts of nearly $43ms^{-1}$.

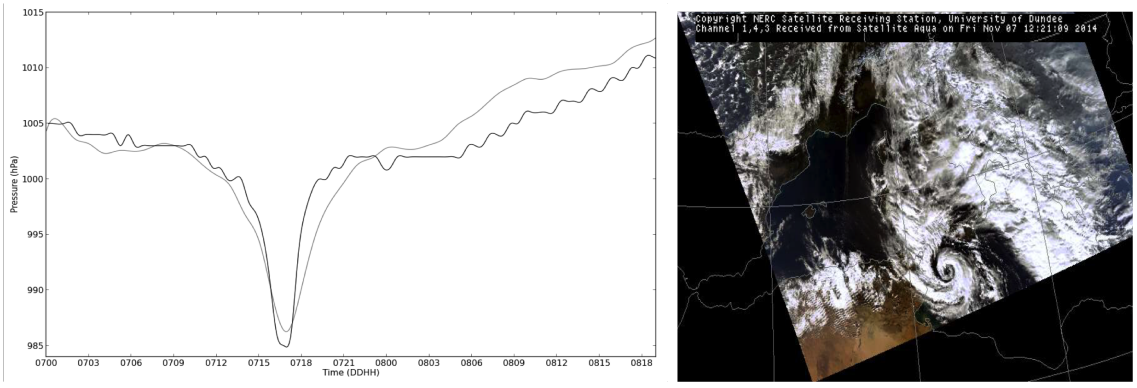

(a) (b)

Figure 1: Observational evidence of the Medicane. (a) Pressure (hPa) record observed in Malta (black) and pressure drop simulated through a model in a deterministic study (grey). Time is indicated as DDHH (day hour) of November 2014. From Carrió et al. (2017). (b) Satellite image of the Medicane on Nov 7 at 12:21 UTC

1.3 Sensitivity: methods and applications

Current predictions of the atmospheric state can very accurately determine what the future weather will be over a time span of days. However, the main weather forecasting centers, which can be taken as a reference, do not match exactly in their predictions. In fact, the conditions they use to initialize the model are not equal either and yet, both predictions have value even if they differ. How can all of these be consistent within a general prediction challenge? The "problem" comes from the atmospheric models. Current atmospheric models have chaotic dynamics and very small differences in the initial conditions can become large differences after a certain simulation time. This is so important that for a long enough forecast integration, the prediction becomes worthless and two states initialized with similar initial conditions differ as much as two random states, as already discussed by Lorenz.

This predictability problem underlies the nature of the models, and can not be escaped or overcome entirely in a deterministic framework. However, it is possible to reduce its impact in specific occasions. If there was a potential extreme weather event, it would be desirable to know beforehand the areas affected in order to warn and protect the population about the potentially devastating effects. Since the nature of the model remains unchanged, the most sensible approach is to have the best field for initial conditions possible, which is highly influenced by the available observations. However, for a particular event (or type of event) a homogeneous increase in the spatial resolution, frequency and accuracy of observations would be a waste of resources and efforts, since most of those barely change the previous estimation of the initial state. This is where the value of sensitivity information comes in.

There are multiple sensitivity calculation methods but they can be classified in the two different approaches they take. In the first approach, used by the factors separation method explained below, a few causes are selected and all of their consequences can be determined. In the second approach, taken by the methods used in this work such as the adjoint model or the probabilistic sensitivities, consequences are selected and all of their causes can be determined.

The first technique explained here and which uses the first approach mentioned is the factor separation technique (Stein and Alpert, 1993). This method relies on a set of numerical simulations where a few selected factors are modified. For the simple case let us assume two factors we determine to be important *a priori*: F1 and F2 (for example, the presence of certain orographic elements and latent heat flux from the sea). Then, with the run of four simulations, it is possible to identify the effect of both of these factors separately and their synergy. A more explicative schematic view of this case with two factors can be seen in figure 2. In the case of a number of factors n, the required number of simulations varies as 2^n, and the interpretation of the combined effects becomes more complex.

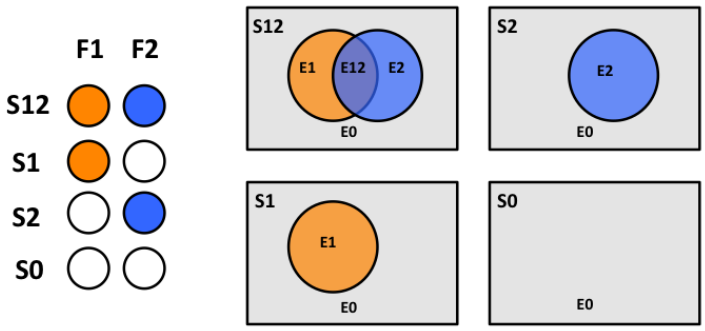

Figure 2: Schematic view of the factors separation technique

Once these simulations are run, it is straightforward to isolate all the effects of interest: both individual effects and the synergy between them. With this purpose, we define the effects $E0$, $E1$, $E2$ and $E12$. The first three variables represent respectively the effect of all the factors except the ones we are taking into account, the individual effect of the first factor and the individual effect of the second factor. The last effect variable represents the effect of the synergy between the two factors considered. Taking all of this into account, expressions for these effects can be extracted from the different simulations:

$$E0 = S0$$
$$E1 = S1 - S0$$
$$E2 = S2 - S0$$
$$E12 = S12 - (S1 + S2) + S0$$

The calculation of these effects completes the factor separation technique for the study of sensitivities. However, this technique can only determine the effect of preset factors to the event that took place and can not be used to determine the areas that affected it the most. This is one of the main differences between the factors separation and the adjoint approach. In factors separation a few causes (e.g. F1 and F2) are selected and all of their consequences can be determined. In the method which will be explained later, the adjoint model, consequences are selected and all of their causes can be determined.

Moving on to the second aforementioned approach, the first step is the identification of the element of interest for the calculation of sensitivities, whether it be the accumulated precipitation or the depth of a cyclone. After the selection of this element of interest in the forecast, the calculation of sensitivities determines which areas this aspect is more affected by. In other words, the result of sensitivity calculation points at aspects of the model initialization data (initial conditions) that, when improved by additional observation information, would improve the forecast of this event the most. This happens because sensitivities are informative of a cause-effect relationship. The calculation of these sensitivities is a complex matter and there is not a unique reference method to do so. However, there are a few methods that can be used for this matter.

Another method, which is probably the most computationally expensive one, is what is called a hammer-like backward approach. The basics of the technique work as follows. First, a response function is selected in a control simulation. Then, the domain of the initial conditions is subdivided in little sections. Then, to check the sensitivity of the response function to each of these little areas, a perturbation is introduced in every area and a simulation is ran. The change in the response function with respect to the control is its sensitivity to the perturbed area. This process is repeated for the whole domain. This method is simple but at the same time can be a big waste of computational resources, since it is likely that simulations are run for perturbed areas of null sensitivity which does not provide much useful information at all.

Another sensitivities calculation method, and one which will be used in this work, is the adjoint model (e.g. Errico 1997, Zhong 2007). This method uses the non-linear model only once. Then, a tangent linear model, which is tangent to the non-linear trajectory at every point of the phase space is calculated. Since the trajectory followed by the tangent linear model is linear, its adjoint can be obtained. The adjoint of the tangent linear model is the adjoint model. The non-linear model takes as initial conditions an atmospheric state and the tangent linear model takes a perturbation to the atmospheric state. However, the input of the adjoint differs quite significantly from the other two. The adjoint model takes as an initiator the sensitivity to a response function and its state variables are gradients with respect to this response function of the tangent linear state variables. This response function can be defined as the forecast characteristic representative of the event of interest. The main limitation of the adjoint model is the restriction imposed by its linear behaviour. This can be a mere characteristic sometimes but a determinant factor other times. For highly non-linear cases, this linear approximation can make the adjoint results effectively useless in realistic fully non-linear applications.

One last method for the calculation of sensitivities is the statistical sensitivities approach. This method makes use of covariance information contained in an ensemble of forecasts. Ensemble prediction systems are the current standard in operational numerical weather prediction offices and provide a finite statistical sample of the distribution of possible atmospheric states compatible with all available information about that state. Ensembles are the current standard to cope with the prediction of the atmospheric state, including the associated uncertainties. Being an ensemble a statistical sample of the evolution of the atmospheric state, synchronous and asynchronous covariances can be easily and affordably produced. Asynchronous covariances provide linear relationship information which is essentially identical in nature to the gradients computed by the adjoint model (Ancell, 2007). The statistical sensitivity approach is also limited by the same linear hypothesis as the adjoint model, and therefore shares a fair amount of its limitations. Furthermore, the statistical approach adds the problem of the misrepresentation of the system in the phase space, where ensemble members are just a finite rank-deficient representation of the actual distribution of possible states.

All of these sensitivities can be used as a method for physical understanding of meteorological phenomena. However, the applications of sensitivities go beyond a mere interpretation of the physical information behind the fields. One of the main uses is its application in what is known as targeting. Targeting works as follows: first, a simulation is ran with its corresponding initial conditions until the verification time when the phenomenon of interest takes place. After this simulation is done, sensitivities are calculated for a selected response function, representative of the event of interest with respect to time t. This time is selected as a time when additional observations could be made in order to improve the forecast, in other words, a time t between the moment when the forecast is produced and the actual occurrence of the event. This time t is called the targeting time, and it is the moment when the new observations can be made. With information about where the largest sensitivities are located, it is possible to make optimal extra observations and improve the knowledge of the state of the atmosphere at those key points, hopefully making the forecast of the phenomenon of interest more precise. There is an underlying problem to this method since the areas of larger analysis uncertainty are not necessarily the areas of larger observation uncertainty and the observation-analysis transformation (which also involves a background field) is not being taken into account. Homar and Stensrud (2008) used a simple masking of the sensitivity field based on the inverse of the observing network density. Other more complex methods such as the Ensemble Transform Kalman Filter (ETKF) account for analysis error when computing sensitivities.

Another use for sensitivities is the adaptation of ensemble prediction systems to particular phenomena of interest. Let us consider a situation where we want to generate an ensemble prediction system for a certain event and we have a set of initial conditions and a sensitivity field for that event at the initial time. With that information in mind, it is possible to adapt the ensemble to the specific uncertainties affecting the phenomena of interest. The generation of new members of the ensemble can be based on the most sensitive areas and therefore, each member will bring more information to the ensemble, covering a bigger variance of possible atmospheric states. A better understanding of this can be achieved thinking of the opposite case. Imagine an ensemble where all new members have been created blindly and their perturbations with respect to the reference initial conditions fall over nearly zero sensitivity zones. Then, that ensemble would be almost useless for the particular mission of forecasting the uncertainties associated with the phenomena of interest, since the changes in the prediction of that phenomenon would be nearly non-existent.

1.4 Previous experiences: ECMWF, MEDEX, FASTEX

The calculation of sensitivities and, specifically, the adjoint model have already been used multiple times and are in constant application. For instance, the European Center for Medium-Range Weather Forecast (ECMWF) has a routinely-used adjoint-based approach to the calculation of Forecast Sensitivity to Observation Impact. The knowledge of the impact observations have in different areas can be applied to targeting. For the ECMWF, knowing the areas with the most relevant observations can be associated with the implementation of targeting campaigns and also with long-term decisions of permanent observation stations. Several projects have applied targeting in more specific cases as well.

The MEDEX (MEDiterranean EXperiment) was a project with the aim of improving the understanding and forecasting of high impact Mediterranean cyclones (Jansà et al 2014). This project consisted of multiple approaches to the study of Mediterranean cyclones, one of which was the use of targeted observations. The most sensitive areas were calculated mostly through the ECMWF singular vectors, which represent the modes of larger growth. A study with computational experiments of multiple cases was run with their sensitivities and verifications. The sensitivities were verified using two methods. The first consisted on introducing artificial perturbations. The second method was more realistic for its proximity to the possible operational application. It consisted on the assimilation of additional observations to the basic set of observations or (in the absence of additional observations) the assimilation of these basic observations in two bagdes, using the second badge as a representation of targeted observations. This way, actual observations were incorporated even if they were not initially obtained using targeting methods. The conclusions of this experiment were that the addition of data can be useful and its contribution is not negligible.

Another experiment which used targeting to try and improve forecasting was the Fronts and Atlantic Storm Track EXperiment (FASTEX). The aim of this project was to improve the prediction of Atlantic cyclones specially with the use of upstream observations (Snyder 1995). The FASTEX experiment initiated a discussion on different sensitivity calculation methods (bred vectors, singular vectors and the adjoint model). This experiment allowed for a more precise understading of frontal cyclones and the underlying physical processes involved in their genesis and evolution.

1.5 Objectives and structure of the document

The aim of this work is divided in two main parts. The first is the calculation of the adjoint sensitivities of the Medicane and their physical interpretation. The second is the verification and test of these sensitivities. With this second objective in mind, two approaches are taken. On the one hand, modifications to the simulation are made in order to understand the role of different processes in the sensitivities results. The control adjoint sensitivities are also compared to sensitivities obtained from a probabilistic clustered ensemble method. On the other hand, a test of linearity is carried out, as linearity is a limiting factor for the adjoint model, sometimes the most important one. Another way to express the objectives of this document is trying to answer two questions: "What are the sensitivities of the Medicane like?" and "Are these sensitivities reliable?".

This document is structured following these objectives. First of all, in section 2 the methodology used is explained. The adjoint sensitivities of the Medicane are shown in section 3. Afterwards, section 4 contains a consistency check of the sensitivities. Linearity checks of the obtained sensitivities are displayed in section 5. Finally, a summary of this work and the general conclusions are presented in section 6.

2 Methodology

2.1 Generation of initial conditions

Nowadays, all predictions of the future state of the atmosphere are made with numerical models as the main tool in what is known as numerical weather prediction. These numerical models need (besides their own physical parametrizations) two input sources: a set of initial conditions and the corresponding boundary conditions in the case of the so-called *limited area* simulations.

Being an initial value problem, solving the set of primitive differential equations, even numerically, requires initial conditions. These are most often the best estimate of the atmospheric state at the simulation start time. The best way to approach these is through a combination of previous model runs (background) with fresh observations. The current most advanced way these informations are incorporated into the background is through data assimilation, which determines the initial conditions. A typical assimilation cycle for a regional forecast (which uses boundary conditions from a global model) is sketched in figure 3.

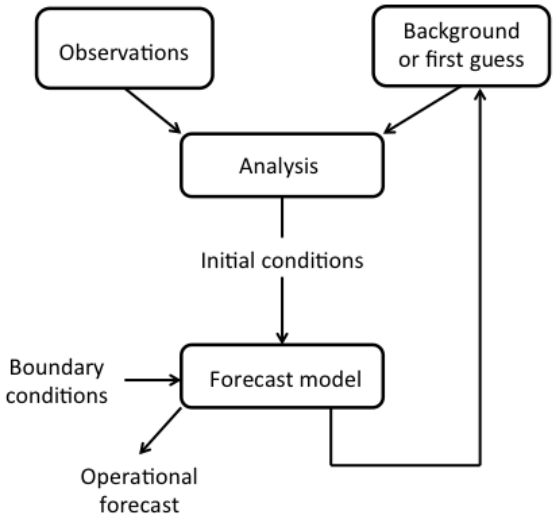

Figure 3: Schematic view of a data assimilation cycle

The unknown quantity now becomes the analysis. In this work two different sets of initial conditions (i.e. analysis) are used, both of them valid for 7 November at 00UTC. The first comes from an assimilation cycle that has ran for 18 hours, which started at 06UTC of November 6^{th} and therefore is valid at 00UTC November 7^{th}. The start of this assimilation cycle was carried out using as the first guess field a downscaling of the ECMWF global model (a member of its ensemble). Since this initial condition has been running for 18 hours and the microphysical species have already developed, this set of initial conditions will be called a warm start.

The other set of initial conditions used is a direct downscaling of the ECMWF deterministic global model at 00UTC of November 7^{th}. This direct downscaling lacks microphysical species,

which is why it is called a cold start. The only microphysical quantity different from zero is the water vapor, all fields referent to clouds or any sort of precipitation are null.

2.2 Adjoint and tangent linear models

The main tool for weather prediction are numerical models. They solve the equations that regulate the atmosphere (dynamics) as well as a set of parameters that control the processes occuring at subgrid scale (physics). These models are non-linear and contain multiple diffusive processes and bifurcation points, which limits the possibility of finding their adjoint them. However, there is a tool that provides information about the adjoint model in a linear approximation: the tangent linear and adjoint models.

The tangent linear model is generated from the non-linear model, and it is defined as the tangent linear operator that simulates the evolution of perturbations following a trajectory tangent to the non-linear model at every point of the phase space. The more linear an ordinary non-linear evolution is, the more accurate the results of this tangent linear model because the real and the tangent linear evolution are more similar. Since the adjoint of all linear operators can be found, it is direct to extract that the tangent linear model has an associated adjoint model.

The three models have different roles and work with different variables. The non-linear model evolves the whole atmospheric state forward in time. The tangent linear model evolves perturbations of the atmospheric state, also forward in time. However, the adjoint model evolves sensitivities backward in time. In other words, the state variables of the adjoint model are the gradients of a response function to the tangent linear state vector, which are evolved back in time, resulting in sensitivities of the response function to perturbations of the basic nonlinear trajectory.

Assuming an initial state of the atmosphere $\vec{x}(t_0)$ and a non-linear model M:

$$\vec{x}(t) = M\vec{x}(t_0) \tag{1}$$

$$\vec{x}(t) + \delta\vec{x}(t) = M\left[\vec{x}(t_0) + \delta\vec{x}(t_0)\right] \tag{2}$$

The evolution of the state itself leads to another state. If this initial state is perturbed, the evolution is different and in general there is not a linear relation between the inital and the final perturbations. Now, let us take a linearization of M, where there will be a linear relation between initial and final perturbation:

$$\vec{x}(t) + \delta\vec{x}(t) = M\left[\vec{x}(t_0)\right] + \frac{\partial M}{\partial \vec{x}}\left[\delta\vec{x}(t_0)\right] + O\left(\delta\vec{x}(t_0)^2\right) \tag{3}$$

where $\delta\vec{x} \approx L\left[\delta\vec{x}(t_0)\right]$ and $L \equiv \frac{\partial M}{\partial \vec{x}}$. Terms of $O\left(\delta\vec{x}(t_0)^2\right)$ and superior will be neglected.

We will define the adjoint model A as the transpose (or adjoint operator) of L, the tangent linear model. In order to do so, it is necessary to first introduce a norm. The euclidian norm, which is defined as the inner product in a Hilbert space, can be written as:

$$||\vec{x}||^2 = <\vec{x}, \vec{x}> = \sum_i x_i x_i \tag{4}$$

Now, with this definition in mind it is possible to define the adjoint model A as the mathematical adjoint of L:

$$< \vec{\chi}, L\,[\delta\vec{x}] >=< A\vec{\chi}, \delta\vec{x} > \tag{5}$$

This $\vec{\chi}$ represents sensitivities, which are inputed to the model at time t and are transported to time t_0. A clear way to see how the adjoint model integrates back in time is through the decomposition of the operators in n different models. Both the non-linear model and the tangent linear model can be decomposed in these successive models, one applied to the state vector and one applied to its perturbation:

$$M\vec{x}(t) = M_n \cdot ... \cdot M_3 \cdot M_2 \cdot M_1\vec{x}(t_0) \tag{6}$$

$$L\delta\vec{x}(t) = L_n \cdot ... \cdot L_3 \cdot L_2 \cdot L_1\delta\vec{x}(t_0) \tag{7}$$

As the adjoint model A is the transpose of L, when considering it as a matrix it can be seen as its complex conjugate. Taking this into account and applying the n models and the complex conjugate properties, it is direct to write:

$$A = L^* = (L_n \cdot ... \cdot L_3 \cdot L_2 \cdot L_1)^* = L_1^* \cdot L_2^* \cdot L_3^* \cdot ... \cdot L_n^* \tag{8}$$

$$\vec{\chi}(t_0) = A_1 \cdot A_2 \cdot A_3 \cdot ... \cdot A_n\vec{\chi}(t) \tag{9}$$

A better understanding of the way this whole system works is through a visual representation (figure 4).

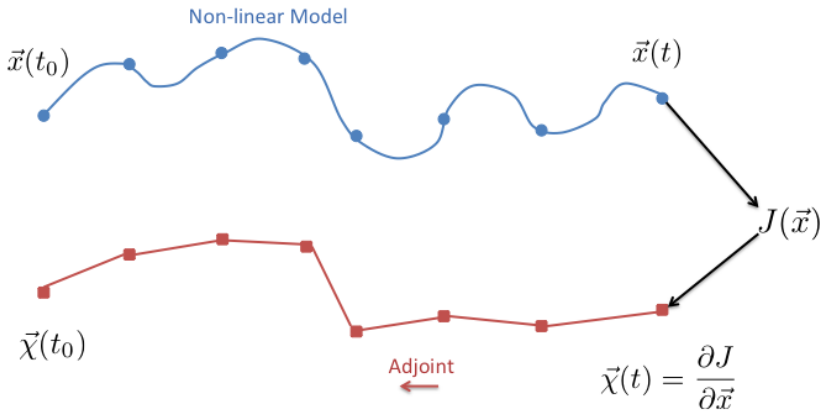

Figure 4: Schematic view of the adjoint model

The definition of the response function which is introduced to the adjoint model is key to the obtained initial sensitivities, since it defines the sensitivities at the final time that are evolved. Many applications of the adjoint model have used the forecast error as the response function in order to determine which areas influence the quality of the prediction the most. However, in this case the selection of a response function representative of the cyclone will be a better option for the study of its formation and characteristics.

2.3 Adjoint simulation setup

The adjoint model used was WRFPLUS, the adjoint of the WRF (Weather Research and Forecasting) Model (Zhang 2013). The simulation started on 00UTC of the 7th of November 2014 and

ran for 12 hours. The boundary conditions were provided every three hours from the ECMWF deterministic global model (nearly 16km horizontal resolution). The grid was established with 200 points in the west-east direction and 165 points in the south-north direction, with 51 vertical levels (unevenly distributed so that the resolution was higher closer to the surface and with a pressure top of 50hPa). The horizontal resolution used is 15km in both directions, which is paired with a time step of 60s. Ideally, the maximum allowed time step to prevent CFL numerical instabilities should be around 90s, but the intensity of some simulated winds did not allow such high time steps. The domain extent can be seen, for example, in figure 5.

Not all the available physical parameterizations in WRF have been activated. For a comprehensive description of the simulation, here is a list of the activated parameterizations: microphysics processes (Thompson scheme), radiation physics (rrtm scheme for long wave and Dudhia scheme for short wave), surface layer physics (with a MYNN surface layer and an Unified Noah land-surface model), planetary boundary layer physics (MYNN 2.5 level TKE scheme), cumulus physics (Kain-Fritsch scheme), heat and moisture fluxes from the surface, snow cover effects and, finally, the cloud effect to the optical depth in radiation (Xu-Randall method). All of these options are relevant to the simulation but in this particular case perhaps the cumulus option is the most relevant. This option covers the parameterization of subgrid cumulus that are not explicitly resolved by the model grid. An important point to add is the option regarding heating from microphysical species. This is activated by default but can be deactivated, an option that is not taken in the control simulation but that will later come in handy.

For a better undertanding of the case, the initial sea level pressure fields for the two initial conditions are shown in figure 5. This knowledge of the initial surface low and where it is located will be useful later in this document, as the location of the sensitivities relative to this low will help give a physical interpretation to the fields.

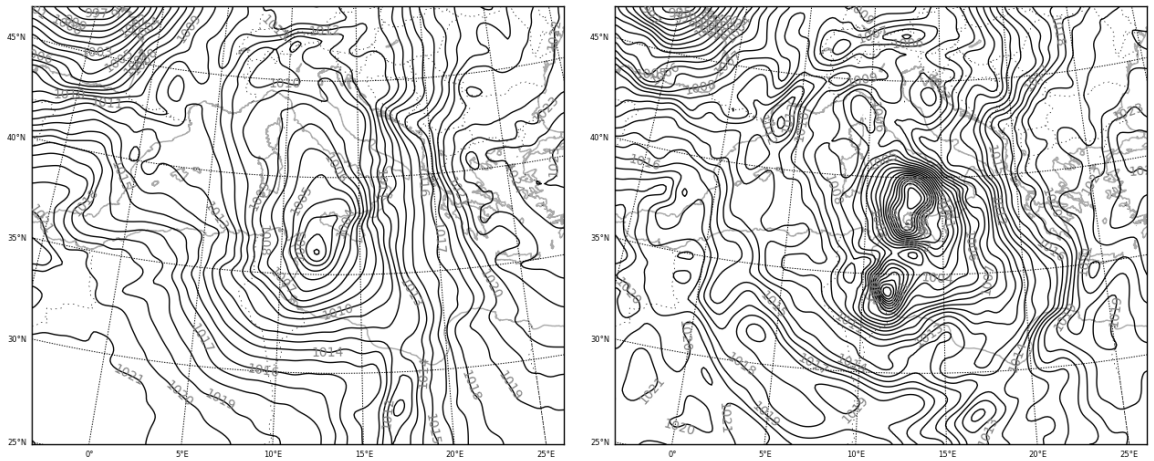

(a) (b)

Figure 5: Initial locations of the sea level pressure lows at 7 Nov 00UTC for (a) the cold start and (b) the warm start. In the warm start,the surface low that later becomes the Medicane is not the largest one, but the small one located on the large bay in the Tunisian coast. Isolines are spaced by 1hPa.

2.4 Clustered ensemble sensitivities

Ensemble forecasting methods are a probabilistic approach to the study of the atmosphere. The scalars that define the state of the atmosphere in a deterministic approach are turned into probability density functions (PDFs) in the probabilistic approach. The ensemble forecasting methods consist of generating a set of numerical simulations (using the complete non-linear model) which are frequently all possible and equally likely. This set of forecasts can then be treated statistically considering each forecast as a sample of the complete PDF, allowing for a wider understanding of the workings of the atmosphere.

It is possible to conduct a sensitivity analysis from this ensemble describing a situation and its set of members. The way this is done is taking all members and looking at some characteristic that is interesting (response function) and seeing how it depends on other functions. It is the possible to create a covariance matrix to see how the variation of the response function between members is related to the variation of other variables. A simplified one-dimensional case can be seen in figure 6a.

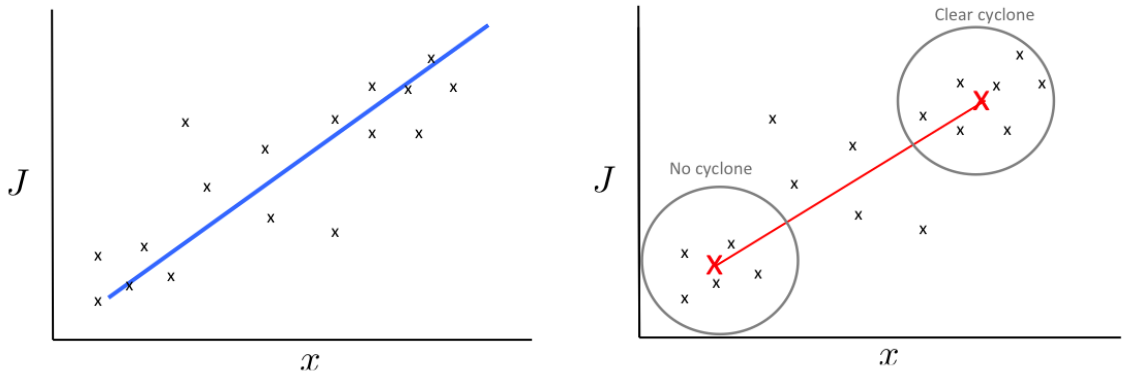

Figure 6: Schematical view of ensemble sensitivities. Comparison of ordinary (a) and clustered (b) methods.

However, the method used in this work will be a new approach derived from this standard ensemble sensitivities method. In this particular case, we are using a 24-member ensemble which was already made. Instead of defining a quantitative response function, a binary clustering will be made into members that form a Medicane (MED) and members that do not (NOM). To compensate the loss of a concrete numerical criterion, multiple qualitative criteria representative of a tropical-like cyclone will be selected. More specifically, an isolated surface low pressure, a relative vorticity maximum and a relatively warm center (looking at equivalent potential temperature). The combination of all three factors will generate a classification of the members. After determining whether an ensemble member has formed a Medicane or not, it will be classified in one of two groups: MED or NOM or will remain unclassified if it is not clear (figure 7).

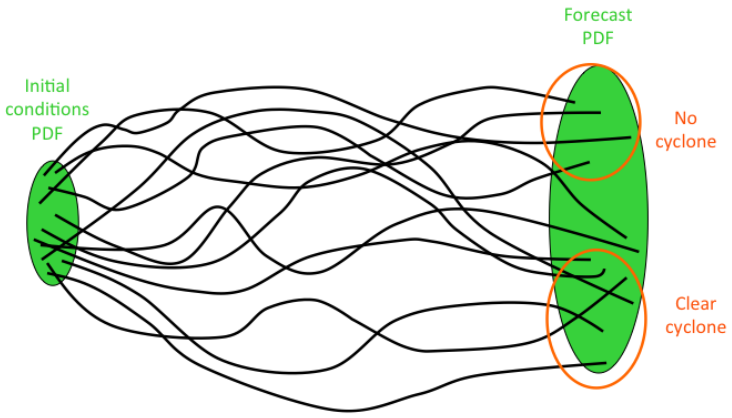

Figure 7: Schematic simplified view of the clustered ensemble sensitivities method

For the clustered ensemble sensitivities method, these two groups MED and NOM are taken. Then, both of them are averaged separately, in order to extract the indentifying properties common to the members of each cluster. Finally, in order to isolate the cyclone-generating factors, the NOM average is substracted from the MED average. This way, the remaining aspects of the different fields are potentially meaningful differences between the members that generate a cyclone and those that don't (figure 6b).

2.5 Verification methods

Sensitivity information is appealing for its large potential in many valuable applications. However, since no current sensitivity calculation method provides perfect results, a verification and test of its limits of application must be performed. Specifically, the adjoint model relies on the linearity of the case, which is its most important restricting factor. Therefore, one may assume that the adjoint sensitivities will be more trustful the more linear the evolution of perturbation in the case is.

A first verification and validation of sensitivities will be done through a comparison of full adjoint results with other sensitivities. This will be done in two parts. The first will be a comparison with the sensitivities results obtained from the other used method: the clustered ensemble sensitivities. This comparison will help understand whether the general structure of the sensitivities is consistent between the different methods. A second validation will be done using simulations with changes in the parameterizations. This will help understand the role of the physical processes behind these parameterizations in the Medicane formation and also check whether the interpretation of the sensitivity fields changes significantly from one set of parameterizations to another.

The second verification and validation of the obtained sensitivities will be done through a linearity check, one of the most limiting factors to the adjoint model. This verification of linearity can be done with two different approaches. The first is through a model verification included in WRFPLUS which checks whether the non-linear and the tangent-linear model match when running with the same perturbation. The initial conditions are perturbed by a set perturbation whose amplitude is changed from $\alpha = 10^{-1}$ to $\alpha = 10^{-11}$, testing all of the intermediate orders of magnitude. The perturbation used is a scaling of this initial conditions field. The tangent linear model is run once for the perturbation as its linear behaviour allows for simple multiplication to obtain all other values whereas the non-linear model is run as many times as perturbations are tested.

The perturbation used is the input state vector reescaled. Once these simulations are run, the equivalent perturbations of the non-linear run and the tangent linear run are compared in order to extract a linearity coefficient. The closer this coefficient is to one, the more similar both of these perturbations are. This coefficient is dependent on the amplitude of the perturbation and the expression for it is:

$$\Phi(\alpha) \equiv \frac{||NLM(\vec{x} + \alpha\Delta\vec{x}) - NLM(\vec{x})||}{||\alpha TLM(\Delta\vec{x})||} \tag{10}$$

Another linearity check can be done checking perturbations "by hand". In this case, a perturbation is selected and then its amplitude is modified to a selection of values. Then, the non-linear model is run for each perturbed set of initial conditions. After this is done two approaches would be possible. The first is to take this perturbation shape and run it through the tangent linear model as well. Then, a perturbation vector can be extracted from both the non-linear run and the tangent linear run. Afterwards, the correlation between these two vectors is calculated for each amplitude. Now, the higher the correlation, the more linear the evolution of perturbations in the non-linear model, and the more robust the adjoint sensitivity fields are. The second approach to dealing with these multiple simulations is by a simple look at how the response function varies with amplitude. If the problem is linear like we assumed, when an amplitude is twice another, the change with respect to control will be twice as well. This is a simpler and more direct approach that can also be an indicator of the linearity of the problem and the value of the calculated sensitivities.

3 Sensitivities results

In this section the complete adjoint sensitivities of the Medicane are studied. These sensitivities are obtained using the full adjoint model with a complete physical parameterization, able to represent all of the processes that take place in the formation of the Medicane.

3.1 Selection of the response function

It can be seen from the definition of the adjoint model that the way the response function (J) is defined is key to the sensitivity fields that are obtained. In this case, the subject of interest is the cyclone and its depth, so the selection of J needs to reflect those qualities. With this in mind, several approaches are taken, trying to explore a range of response functions and looking for their similarities and differences.

The first and simplest approach is to take J as the pressure at an area surrounding the cyclone center. By taking an area around the cyclone center and not the central point we increase the significance of the resulting sensitivity field by averaging out singularities of individual points. So, in this case, J is taken as the pressure in a prism formed by a square of 9 by 9 horizontal gridpoints (135 by 135 km) and the 4 lowest vertical levels excluding the lowest level, corresponding to the surface, centered over the low-level pressure minimum. This is a very simple approach to the definition of J, but also quite an effective one. For a better understanding of the result, all Js will be expressed as "average response function over the prism".

The second J is taken as pressure over that same area but modulated through a cosine function. This gives more importance on the resulting sensitivity fields to the pressure at the center of the cyclone and lowers the weight of peripheric points.

The third definition of J is taken as relative vorticity over the same prism. The fourth and last definition of J is a specific weighted variation of dry total energy. Taking the definition of this weighted dry total energy as $E \approx T^2 + u^2 + v^2$, where u (ms^{-1}) is the longitudinal wind component, v (ms^{-1}) is the meridional wind component and T (K) is the temperature anomaly with respect to $300K$.

The first three defined Js represent different variants of cyclone intensity. Weighted total dry energy also is representative of cyclone intensity but is harder to interpret than the other two because of its intrinsec non-linearity and the important role played by thermal effects. Being the gradients of the response function the variables of the adjoint model, the input taken by the model for the response function is not J but its derivative with respect to the state vector (sensitivities at the final time). To see the shape this takes, the best way is to take each case and look at it individually. The common aspect of all of the response functions is the area where they are defined, a square prism. Defining i as the west-east coordinate, j as the south-north and k as the vertical coordinate, the prism can be defined as the area compressed between an initial and a final value in the direction of each coordinate.

The response functions that depend on pressure are analyzed first. The prism of interest is limited by i_{st}, j_{st}, k_{st} and i_{end}, j_{end}, k_{end}. In the case of the cosine-moduled response function, i_c and j_c will be the indexes for the central points in the horizontal plane and x_c and y_c will be the geographical coordinates of the central points. The cosine is moduled so that it is zero in the points of the prism furthest from the center (which are separated a distance d_{max} from it) and factor of

$\pi/2$ is included to make the cosine null at these furthest points. Also, it is important to notice that the factor 64 that appears is nothing other than $2d_{max}$ measured in gridpoints.

$$J_1 = \frac{1}{N}\sum_{prism} p = \frac{1}{N}\sum_{i=ist}^{iend}\sum_{j=jst}^{jend}\sum_{k=kst}^{kend} p_{i,j,k} \tag{11}$$

$$\begin{aligned} J_2 &= \frac{1}{N}\sum_{prism} \cos\left(\frac{\pi}{2d_{max}}\sqrt{(x-x_c)^2+(y-y_c)^2}\right) p = \\ &= \frac{1}{N}\sum_{i=ist}^{iend}\sum_{j=jst}^{jend}\sum_{k=kst}^{kend} \cos\left(\frac{\pi}{64}\sqrt{(i-i_c)^2+(j-j_c)^2}\right) p_{i,j,k} \end{aligned} \tag{12}$$

However, the adjoint model variables are not this J function but its derivative with respect to the state vector $\vec{x}$ variables. Taking this derivative for these two cases, the following results are obtained (where var is the state vector variable):

$$\frac{\partial J_1}{\partial \vec{x}} = \begin{cases} \frac{1}{N}, & \text{if } ist, jst, kst \le i,j,k \le iend, jend, kend \text{ and var} = \text{p} \\ 0, & \text{otherwise} \end{cases} \tag{13}$$

$$\frac{\partial J_2}{\partial \vec{x}} = \begin{cases} \frac{1}{N}\cos\left(\frac{\pi}{64}\sqrt{(i-i_c)^2+(j-j_c)^2}\right), & \text{if } ist, jst, kst \le i,j,k \le iend, jend, kend \text{ and var} = \text{p} \\ 0, & \text{otherwise} \end{cases} \tag{14}$$

The third selected response function is the relative vorticity. The way the grid is defined simplifies the calculations, since $\Delta x = \Delta y = \Delta$:

$$\begin{aligned} J_3 &= \frac{1}{N}\sum_{prism} \zeta = \sum_{prism} \frac{v_{i+1,j,k} - v_{i-1,j,k}}{2\Delta x} - \frac{u_{i,j+1,k} - u_{i,j-1,k}}{2\Delta y} = \\ &= \frac{1}{2N\Delta}\sum_{i=ist}^{iend}\sum_{j=jst}^{jend}\sum_{k=kst}^{kend} [v_{i+1,j,k} - v_{i-1,j,k} - u_{i,j+1,k} + u_{i,j-1,k}] \end{aligned} \tag{15}$$

$$\frac{\partial J_3}{\partial \vec{x}} = \begin{cases} 1/2N\Delta, & \text{if } ist+1, jst, kst \le i,j,k \le iend+1, jend, kend \text{ and var} = \text{v} \\ -1/2N\Delta, & \text{if } ist-1, jst, kst \le i,j,k \le iend-1, jend, kend \text{ and var} = \text{v} \\ -1/2N\Delta, & \text{if } ist, jst+1, kst \le i,j,k \le iend, jend+1, kend \text{ and var} = \text{u} \\ 1/2N\Delta, & \text{if } ist, jst-1, kst \le i,j,k \le iend, jend-1, kend \text{ and var} = \text{u} \\ 0, & \text{otherwise} \end{cases} \tag{16}$$

The final selected response function is the weighted total dry energy:

$$J_4 = \frac{1}{2N}\sum_{prism} T^2 + u^2 + v^2 = \frac{1}{2N}\sum_{i=ist}^{iend}\sum_{j=jst}^{jend}\sum_{k=kst}^{kend} T_{i,j,k}^2 + u_{i,j,k}^2 + v_{i,j,k}^2 \tag{17}$$

$$\frac{\partial J_4}{\partial \vec{x}} = \begin{cases} T/N, & \text{if } ist, jst, kst \le i,j,k \le iend, jend, kend \text{ and var} = \text{T} \\ u/N, & \text{if } ist, jst, kst \le i,j,k \le iend, jend, kend \text{ and var} = \text{u} \\ v/N, & \text{if } ist, jst, kst \le i,j,k \le iend, jend, kend \text{ and var} = \text{v} \\ 0, & \text{otherwise} \end{cases} \tag{18}$$

This selection of derivatives of the response function is then the initial state of the adjoint model. Of course, this is taken at the final time of the simulation, when the cyclone is at its most intense stage. Then the model will take it back in time and calculate the sensitivities to the initial condition.

An illustrative way to understand these response functions is through a visualization of the shape of their derivatives. Horizontal cuts are shown for non-zero derivatives of the response functions. The sections displayed are representative of all the levels where the derivative is not null for the corresponding vairable since there is no vertical dependence in J (except for J_4, where it depends on the temperature and wind fields). Furthermore, the scaling of these final sensitivities will omit the division by the number of points in order to obtain more intuitive values. Firstly, the derivative with respect to pressure field of the two pressure response functions can be seen in figure 8. In this case, the derivative with respect to pressure is the only one that has values different from zero. It is important to notice that these response functions are valid only for the cold start case and in each different case the corresponding square will be centered over the sea level pressure minimum representative of the cyclone center.

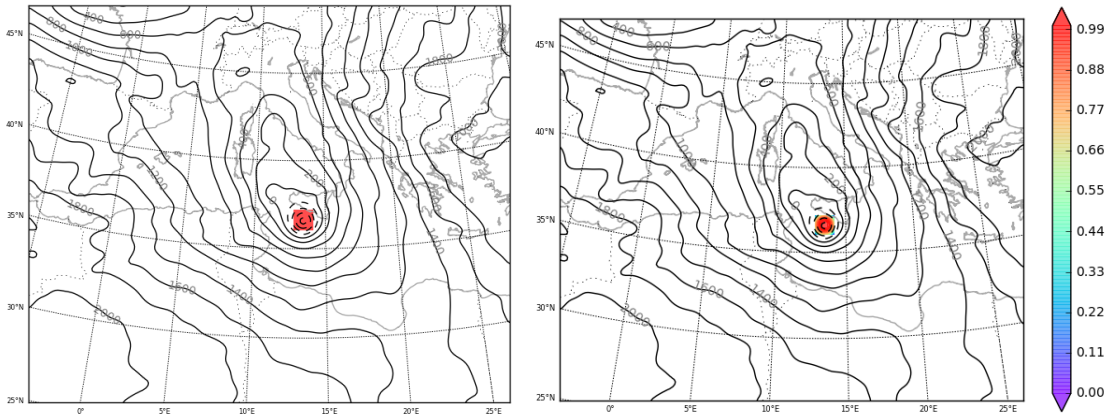

(a) (b)

Figure 8: Derivative of the (a)J_1 and (b)J_2 response functions with respect to the pressure field. All other fields are null. Valid for 7 Nov at 12UTC.

Differently from the pressure response functions, the relative vorticity response function needs two different fields (figure 9) to fully show the shape the derivative takes.

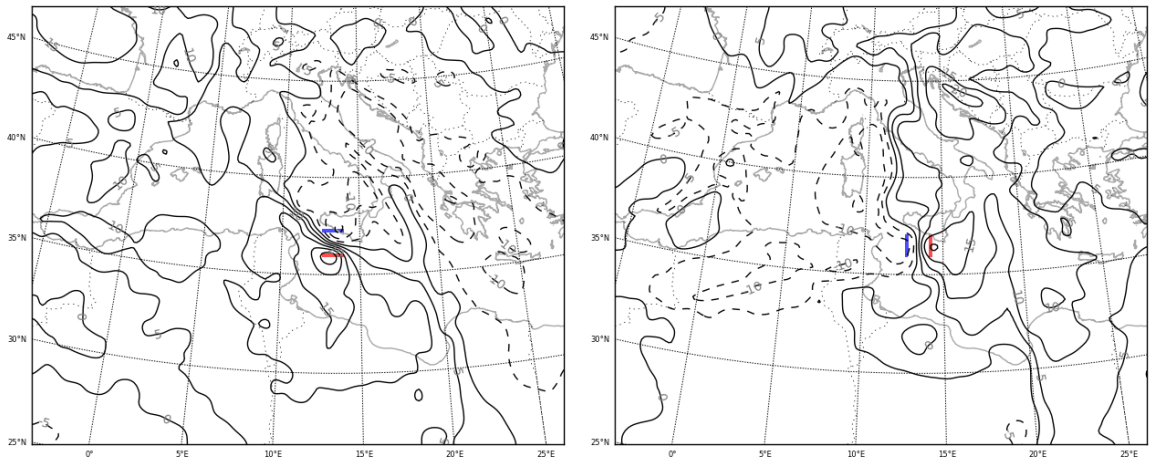

(a) (b)

Figure 9: Derivative of the J_3 response function with respect to (a) the u wind component and (b) the v wind component. All other fields are null. Valid for 7 Nov at 12UTC.

The case of the weighted total dry energy is even more complex, since it needs three fields to show the totality of the derivatives (figure 10). To make things even more complex, this response function is non-linear and thus each field of derivatives corresponds to the variable in the previously defined area.

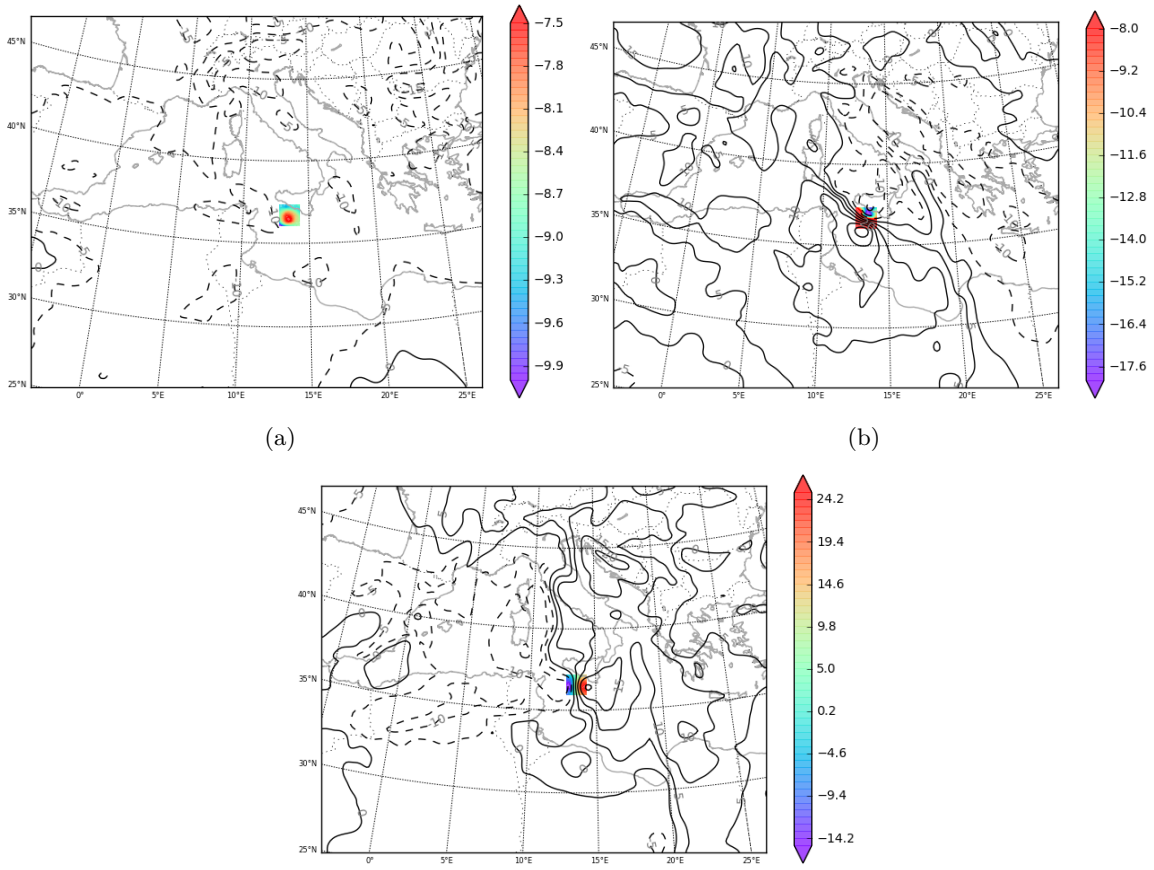

Figure 10: Derivative of the J_4 response function with respect to (a) the temperature anomaly with respect to 300K field (K), (b) the u wind component (ms^{-1}) and (c) the v wind component (ms^{-1}). All other fields are null. Valid for 7 Nov at 12UTC.

3.2 Adjoint sensitivities and interpretation for the cold start

The fields obtained from the adjoint sensitivities approximation (i.e. the use of the adjoint model) represent just a numerical result of the application of a model. Its understanding and interpretation relies fully on the users of these results. It it possible that sometimes the model might give results that are not physical, specially for the microphysical species fields, and it is up to the user to verify these results to test whether they are appliable in that particular case or not. For example, it is possible to have non-zero sensitivity fields to a quantity variable (amount of vapor, ice...) that is null all over the domain. This case would make for a simple interpretation one way (an increase on that variable would increase the response function) but for an impossible interpretation the other way around (it is impossible to have a negative amount of vapor in the air).

In order to check the consistency (or inconsistency) of the sensitivity fields, the way this section is structured depends on the sensitivity field, not on the response function. This way, sensitivities to the same variable with different response functions are grouped together, which allows for a comparison of all the response functions representative of the cyclone.

Before analyzing the sensitivity fields, an important clarification needs to be made. All of the response functions selected represent the intensity of the cyclone in their own way, even though the

weighted total dry energy gives more importance to temperature. The relative vorticity and the energy increase with a more intense cyclone. However, the two response functions depending on pressure decrease when cyclone intensity increases. This is important because "equivalent" sensitivities will have the sign reversed in the two types of cases. The sensitivity fields are represented with their correponding units ([Response function]/[Variable]).

The first field to look at is temperature. What can be seen is a dipole of positive and negative temperature sensitivities. The best way to understand this case is using cyclone intensity as a referent instead of any particular field. This way, the sign present in the pressure dependent response functions can be ignored.

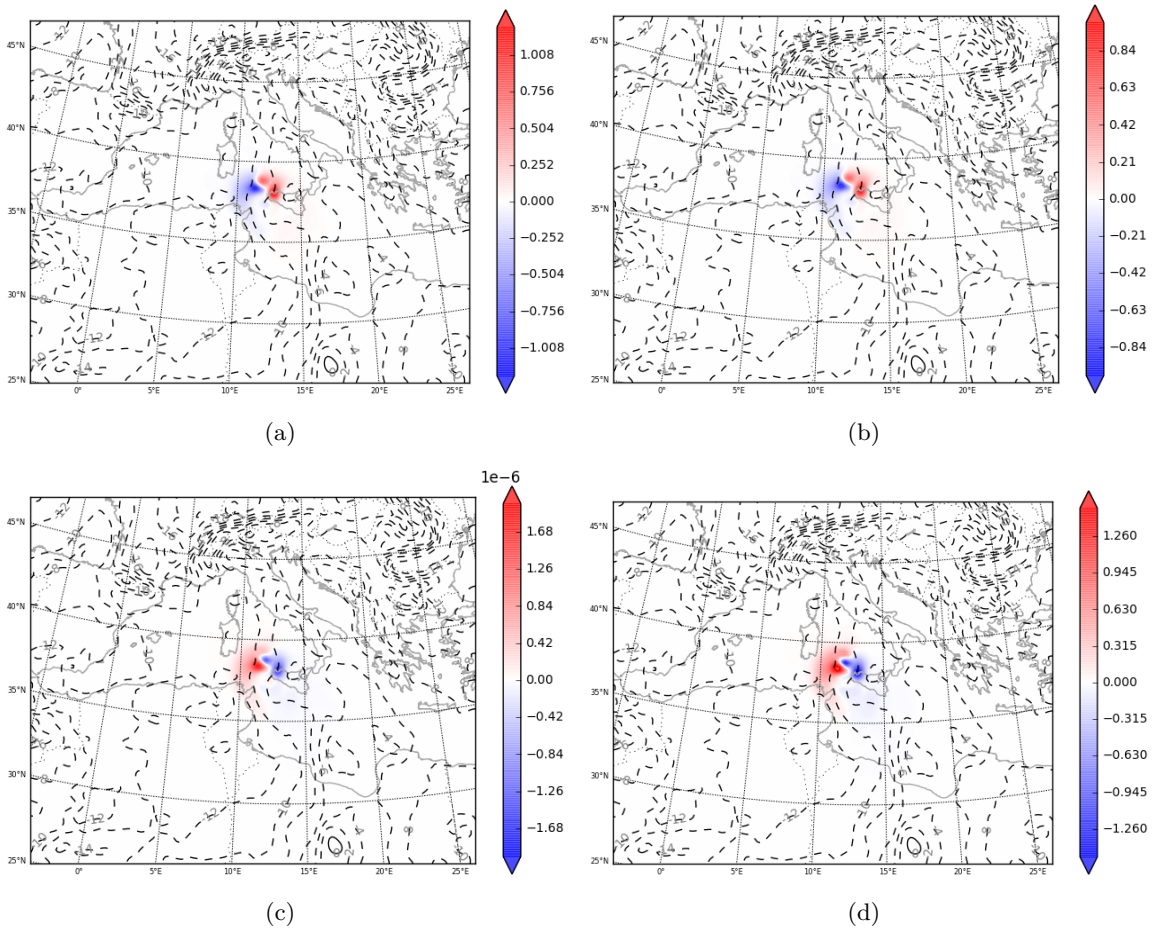

Figure 11: Vertically averaged sensitivity to temperature for a cold start of (a) J_1 (Pa/K), (b) J_2 (Pa/K), (c) J_3 (s^{-1}/K) and (d) J_4 (J/K). Sensitivities are valid for 7 Nov at 00UTC.

All adjoint sensitivities to temperature (figure 11) indicate that if the isolines to the north-west of Sicily were closer to one another (i.e. an intensification of a thermal front occurred) and made a twist, with warmer temperatures in the west and colder ones on the east, the cyclone would have been more intense. At that point, the surface low was located at the southern part of the positive sensitivity area. A part of the intensification could be due to warmer temperatures where the shallow low is located at that point and colder temperatures to the east of it, where it will move later. Since this case is that of a warm-core cyclone, the gradient between the warm nucleus and the exterior favor the Medicane.

Another interesting field to look at are the horizontal wind velocities. In this case longitudinal and meridional components of wind can be seen separately in order to isolate their effects.

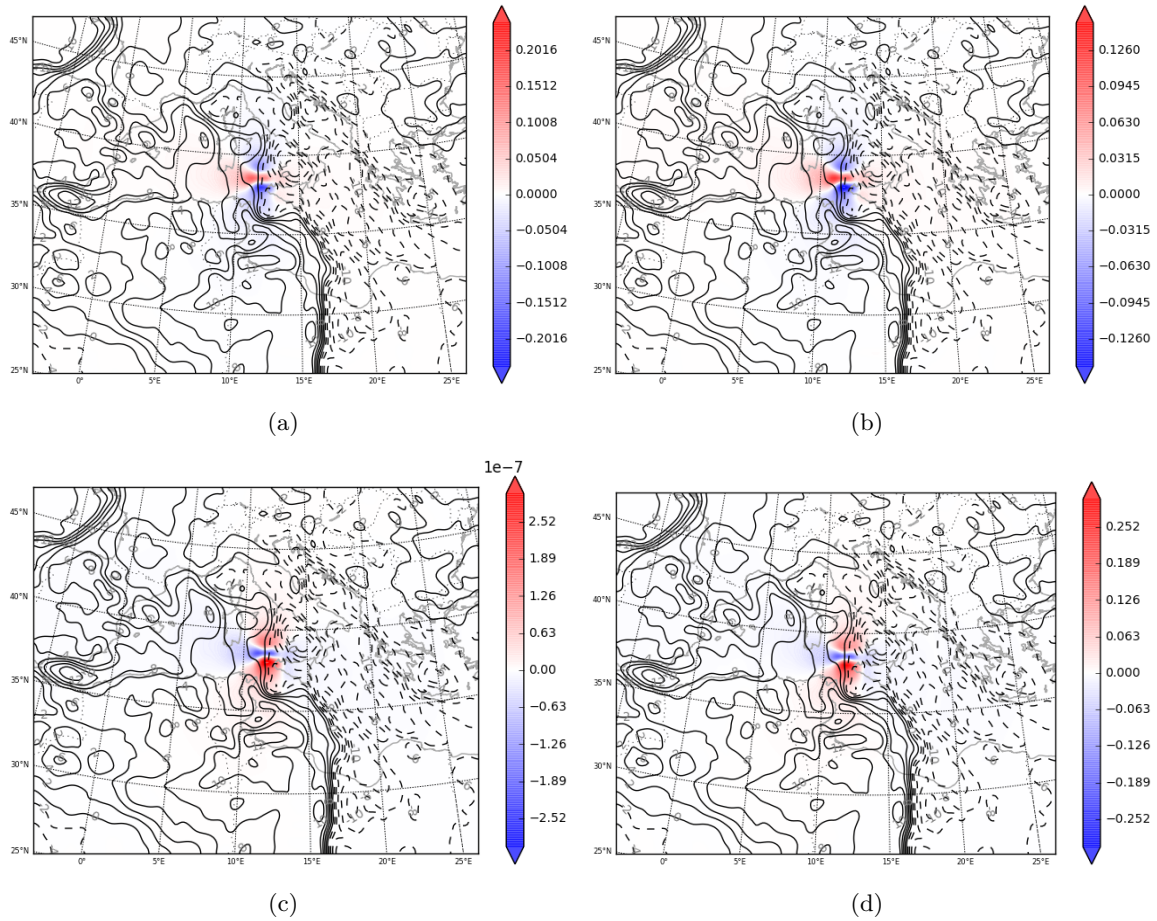

Figure 12: Vertically averaged sensitivity to the u wind component for a cold start of (a) J_1 (Pa/ms^{-1}), (b) J_2 (Pa/ms^{-1}), (c) J_3 (s^{-1}/ms^{-1}) and (d) J_4 (J/ms^{-1}). Sensitivities are valid for 7 Nov at 00UTC.

The largest sensitivities to the u wind component (figure 12) are located at a similar location than the temperature sensitivities. However, this area seems to be larger and instead of a dipole, the sensitivities form a tripole, with a positive-negative-positive structure in the south-north direction. The bottom negative-positive dipole fits over the area of the low pressure at that moment. The southern part of the tripole would suggest that, intensifying the cyclonic circulation at 00UTC to the north of the already existent low-pressure system would intensify the Medicane at 12UTC. The interpretation for the northern sensitivity signals in figure 12 is more speculative but could be related to the positive contribution to the intensification of the Medicane an effective isolation of the southern cyclonic area would have.

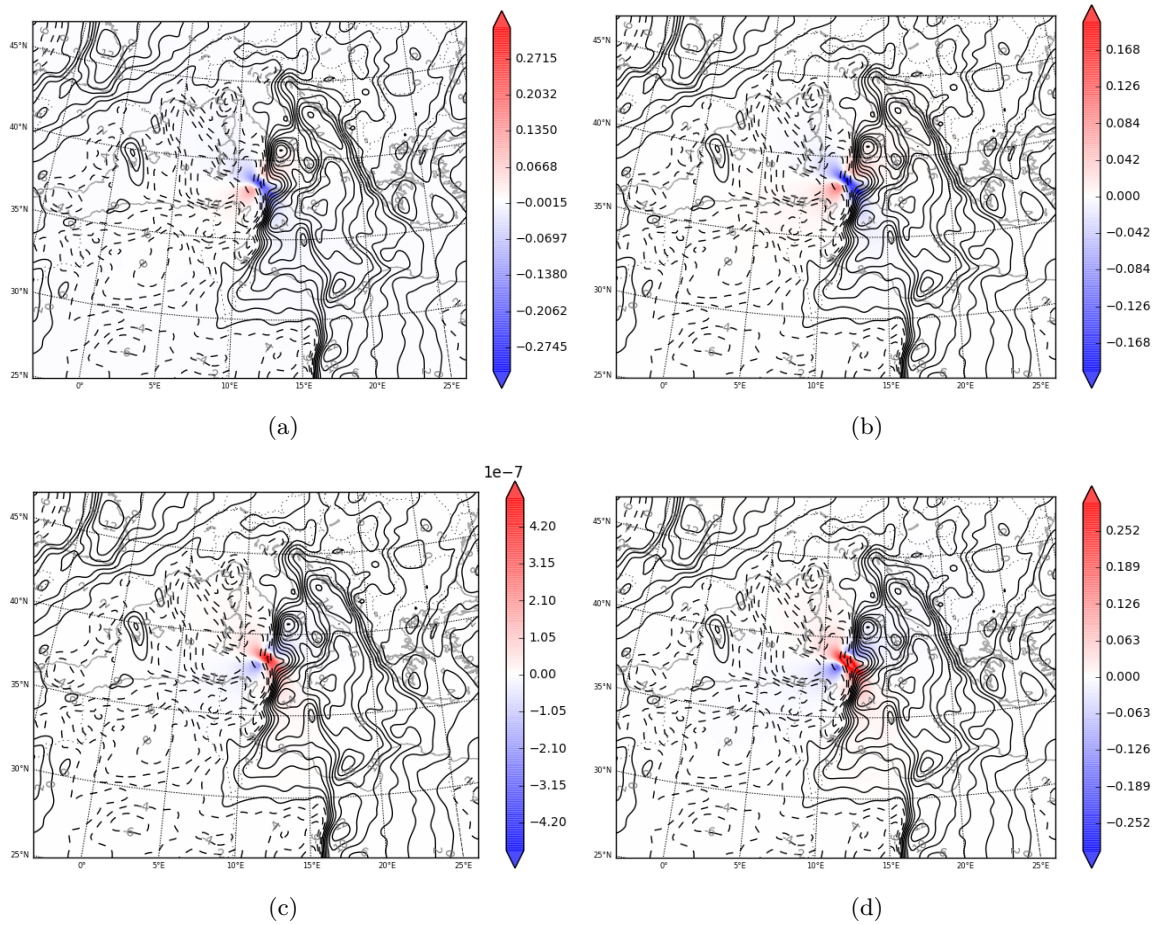

Figure 13: Vertically averaged sensitivity to the v wind component for a cold start of (a) J_1 (Pa/ms^{-1}), (b) J_2 (Pa/ms^{-1}), (c) J_3 (s^{-1}/ms^{-1}) and (d) J_4 (J/ms^{-1}). Sensitivities are valid for 7 Nov at 00UTC.

The structure of the sensitivity fields to the v wind component (figure 13) is similar to that of the u wind component but with a different orientation. It is almost perpendicular to the front and also has the shape of a tripole. This front is a line of wind shear, since the eastern side has winds from the south whereas the western side has them from the north. Again, there is a simple interpretation of the westernmost dipole, since the shear to the north of the surface low would be displaced. This would increase the cyclonic circulation already present in that area. There is a very intense gradient of positive v wind speeds in that area, whose smoothing would favor the formation of a more intense Medicane at 12UTC.

3.3 Adjoint sensitivities and interpretation for the warm start

The same set of adjoint sensitivities were calculated for the warm start run. Again, sensitivity to all four considered response functions is shown in order to test the consistency of the adjoint model results. However, these response functions are moved over the corresponding cyclone center, which is different from the previous one. A first consistency check reveals that the differences in the initial (and also forecast) fields produce fairly significant differences in the sensitivity results, questioning the robustness (and so applicability) of the adjoint fields. It is noteworthy that the warm start sensitivity fields point directly towards the location in the initial conditions

of the center of the seminal cyclone that derived in the formation of the Medicane some hours later.

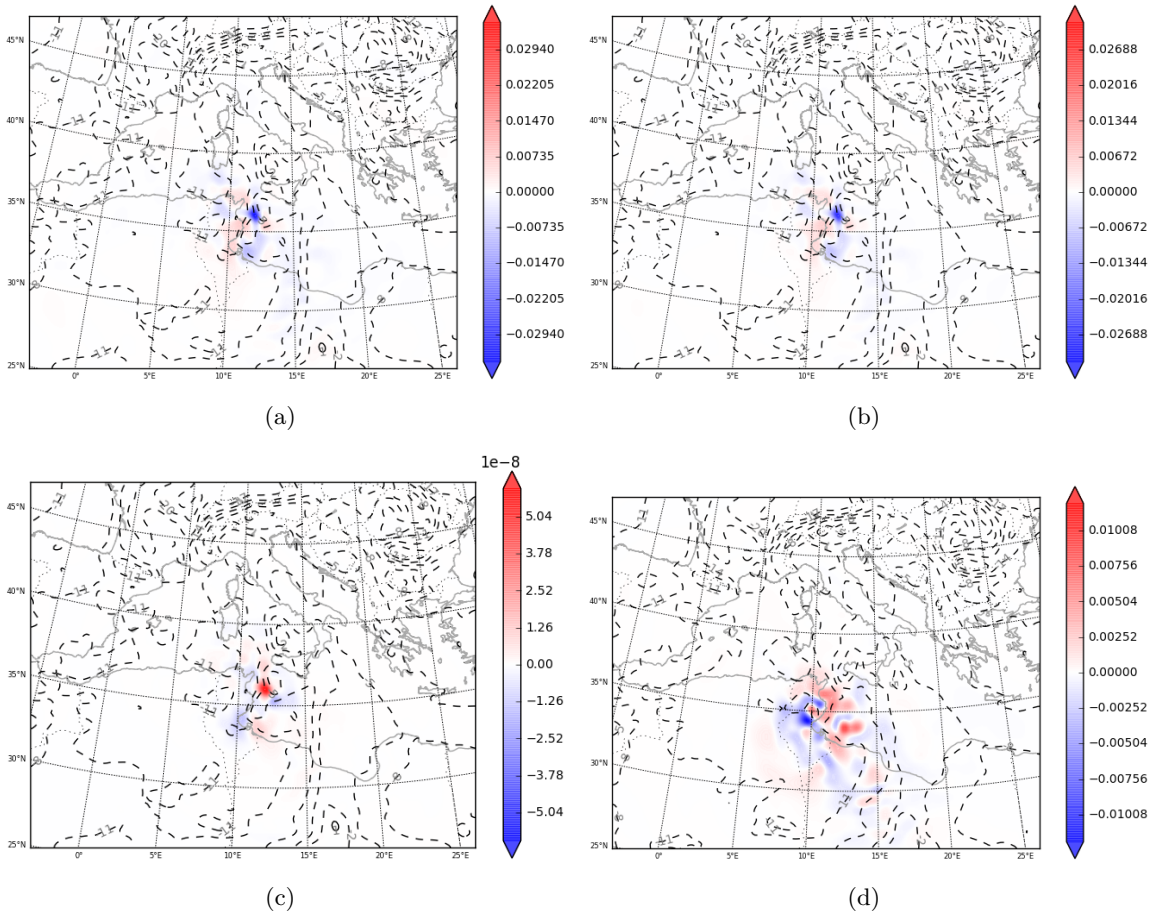

Figure 14: Vertically averaged sensitivity to temperature for a warm start of (a) J_1 (Pa/K), (b) J_2 (Pa/K), (c) J_3 (s^{-1}/K) and (d) J_4 (J/K). Sensitivities are valid for 7 Nov at 00UTC.

Looking firstly at sensitivity to temperature (figure 14), J_1, J_2 and J_3 show very similar structures because all of them represent cyclone intensity directly. The main shape is a positive sensitivity nucleus (with respect to cyclone intensity) located east of Tunisia. This would represent a westward movement of the higher temperature isotherms in that area. The area which would become warmer is located at the center of the sea level pressure isolated low which later becomes the Medicane. In other words, a warmer cyclone center at 00UTC would end up intensifying the Medicane at 1200UTC. This is consistent with the general understanding of Medicane properties, where the latent heat release generates a warm center and therefore intensifies the cyclonic structure.

The sensitivity of J_4 to temperature shows a more complicated structure. It has high values for sensitivity (positive and negative) spread over a larger area. However, the central area to the surface low remains in a positive sensitivity nucleus, indicative again of how a warm center favors cyclone intensity. The negative sensitivity area over Tunisia most likely favors a more intense thermal gradient around the cyclone center, intensifying the warm-core effect. The rest of the sensitivity field has no clear physical interpretation but the general presence of intense positive sensitivities to the north of intense negative sensitivity areas indicate that a decrease in baroclinicity would favor a cyclone of higher weighted total dry energy.

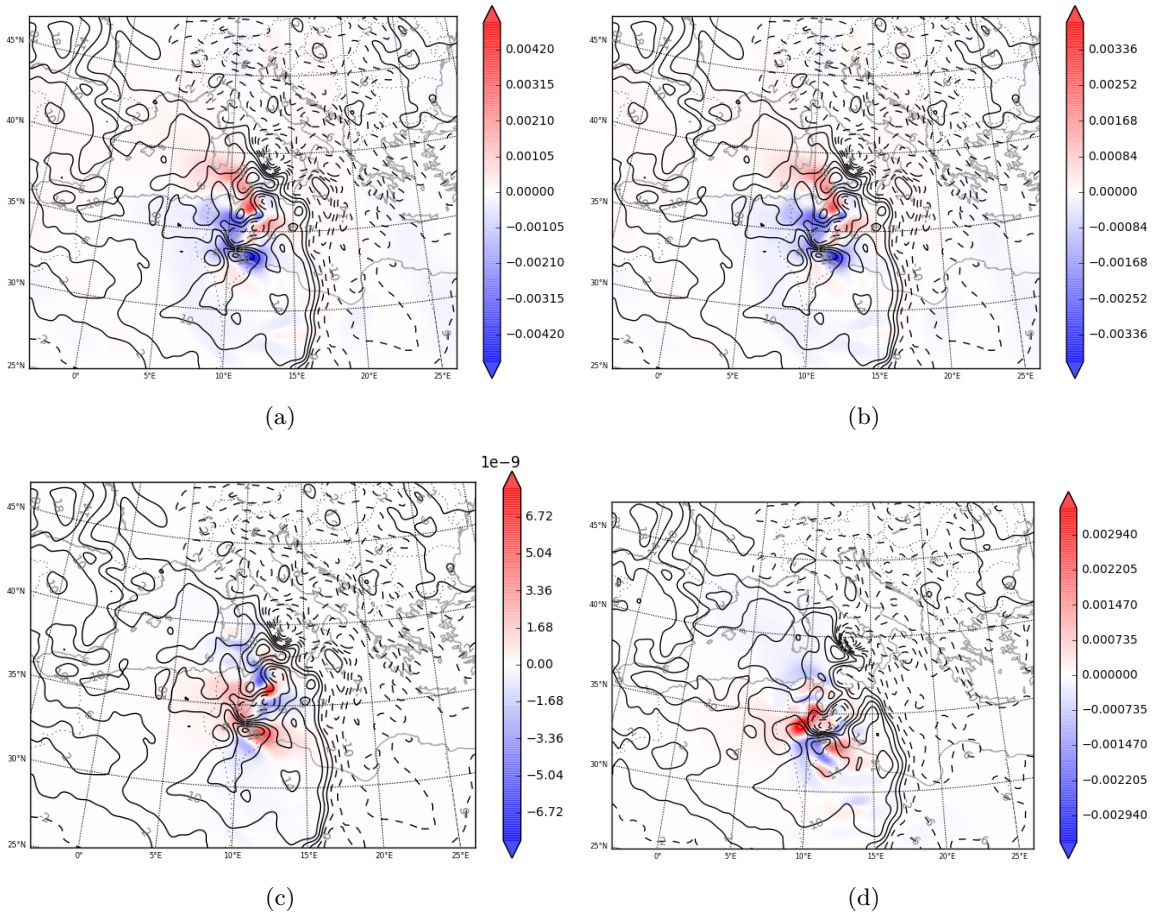

Figure 15: Vertically averaged sensitivity to the u wind component for a warm start of (a) J_1 (Pa/ms^{-1}), (b) J_2 (Pa/ms^{-1}), (c) J_3 (s^{-1}/ms^{-1}) and (d) J_4 (J/ms^{-1}). Sensitivities are valid for 7 Nov at 00UTC.

Looking now at the sensitivities to the zonal wind component (figure 15), the pressure and vorticity response functions show again the exact same behaviour. The most intense dipole, located just east of the Tunisian coast can be clearly related to the shape shown by the isolines. The u wind field shows a negative-positive dipole (negative northern of positive) at the east of Tunisia, which matches the dipole formed by the sensitivities. This expresses that an intensification of this velocity dipole would favor the intensification of the cyclone. This can be attributed to an intensification of the cyclonic circulation already present. The rest of the sensitivity field indicates that a smoothing of the rest of the u wind component field, specially to the north of the cyclonic area would favor the cyclone.

The case of the weighted dry total energy sensitivity to the u wind component is again different from the rest of sensitivities to zonal wind. The same dipole shown in the rest of response functions appears but it is significantly less intense in this case. However, it is also associated with a structure in the wind field. The rest of sensitivities are less straightforward to interpret, but there seems to be an indication that if the initial cyclonic circulation had been more isolated, the Medicane at 12UTC would have been more intense.

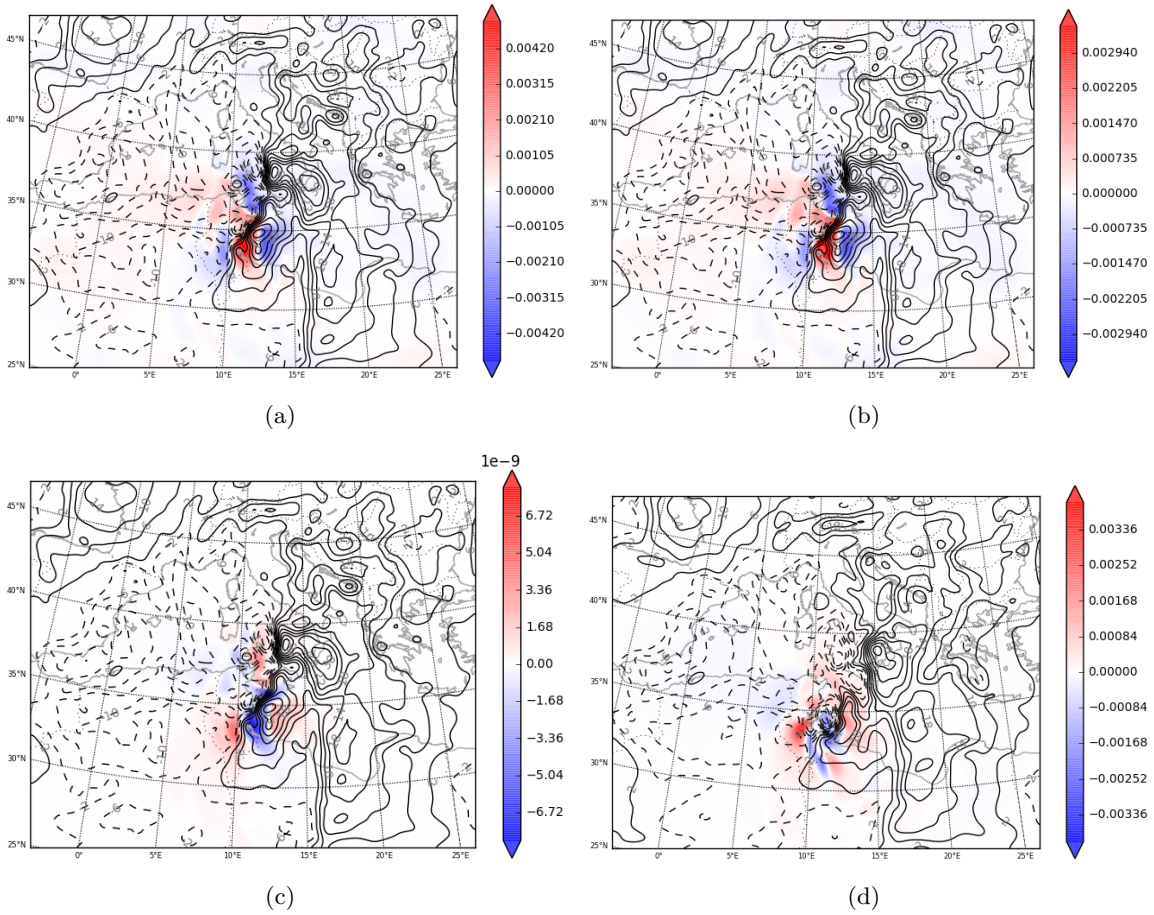

Figure 16: Vertically averaged sensitivity to the v wind component for a warm start of (a) J_1 (Pa/ms^{-1}), (b) J_2 (Pa/ms^{-1}), (c) J_3 (s^{-1}/ms^{-1}) and (d) J_4 (J/ms^{-1}). Sensitivities are valid for 7 Nov at 00UTC.

For the sensitivities to the meridional wind component (figure 16), J_1, J_2 and J_3 show similar structures but their relative intensity varies. However, they agree in a few sensitive aspects of the v field. The three of them show a negative-positive (negative western of positive) dipole just to the east of the Tunisian coast. This indicates that an intensification of the cyclonic circulation around the sea level pressure low would help intensify the Medicane. The rest of the sensitivity structure to the north of this dipole indicate that a westward movement of the shear line would be favorable to Medicane deepening.

The sensitivity of the weighted total dry energy to the v wind component shows different structure to the other response functions, but the general information it provides is quite similar. The dipole with negative sensitivities to the west and positive sensitivities to the east is present to the east of the Tunisian coast, representative that an increased cyclonic circulation at 00UTC would favor the Medicane formation. However, a nucleus of positive sensitivity is located west of the negative pole, whose role might be to isolate this cyclonic circulation.

4 Consistency check of sensitivities

For a validation of the adjoint sensitivities, two different approaches are taken. Firstly, a clustered sensitivities method is used and its results are compared to the previous control adjoint sensitivities. This comparison is used as a validation of the adjoint sensitivities results. The second approach applied is the calculation of adjoint sensitivities with modified parameterizations. Two different experiments will be done for this second approach in order to study the impact of cumulus parameterization and the release of latent heat. It is important to point out that all of the adjoint experiments in this section use the cold start as initial conditions, since no representative differences related to the presence of microphysical species are found in the sensitivity fields between both initial conditions.

4.1 Clustered ensemble sensitivities

The application of the clustered ensemble sensitivities allows for a comparison of sensitivities results with different methods, therefore ruling out a spurious dependence on the method. The initial ensemble was formed by 24 members which had been running an assimilation cycle for 18 hours, equivalently to the warm start initial conditions (which are one of these 24 members). After the classification, the two clusters representative of the method were differentiated. The cluster of Medicane-forming members (MED) was formed by 12 members, six members were introduced into the no-Medicane group (NOM) and six remained unclassified, and thus were discarded. For the sensitivities, the members of MED were averaged in order to extract their common characteristics and the same was done also for NOM. Then, the NOM average was substracted from the MED average, revealing cluster averaged differences in the initial conditions between MED and NOM that must contain key sensitive information about the necessary ingredients in the initial fields at 00UTC for Medicane formation and maturing at 12UTC (figure 17).

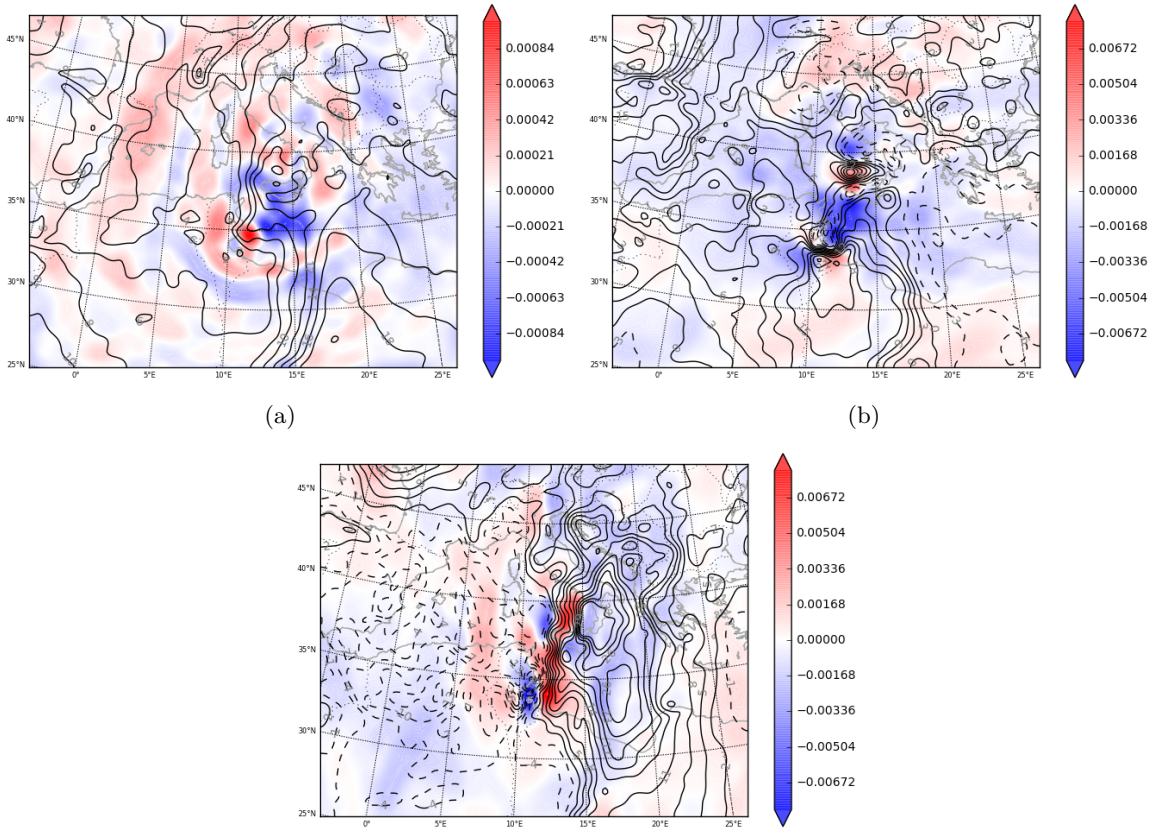

(a) (b)

(c)

Figure 17: Clustered ensemble sensitivities to (a) temperature, (b) the u wind component and (c) the v wind component. Sensitivities are valid for 7 Nov at 00UTC at 850hPa.

The sensitivity to temperature (figure 17a), shows a large negative sensitivity area to the south and west of Sicily and a positive sensitivity area to the east of Tunisia. The positive sensitivity area corresponds with the location of the cyclone at 00UTC, which indicates that warming this area would favor the genesis of the Medicane. Overall, the sensitivity field indicates that, except for the core of the cyclone, an environment with reduced thermal gradients (reduced baroclinic instability) would favor the local intensification of the Medicane.

In the case of sensitivity to the u wind component (figure 17b), there is a dipole of northern negative sensitivity and southern positive sensitivity located on the area where the surface low is located at 00UTC. This is an indicator that a more intense cyclonic circulation slightly displaced to the east would have favored the creation of the Medicane at 12UTC. Also, there is an inverse less intense dipole located to the west of this cyclonic one. This structure indicates that a more isolated cyclonic circulation would be even more favorable to the cyclone formation.

The sensitivities to the v wind component (figure 17c) have a clear physical interpretation. There is a clear division between the east and the west half of the cyclone. The sensitivity field shows a clear dipole in the meridional axis of the preexisting cyclone, and the formation of the Medicane would be favored mainly by a more intense cyclonic circulation around the precursing environment around the Medicane genesis.

These resulting fields of the clustered method show high sensitivities located in areas which can

not affect the cyclone, since in the 12 hours from the initial conditions to the actual Medicane these zones are too far away from the cyclone to influence its formation. This is due to the presence of structures in both average fields that can not be associated to a cause-effect relation.

4.2 Impact of parameterized convection on adjoint sensitivities

When looking at these sensitivities, it is important to keep in mind that the only change from the already calculated complete sensitivities is the parameterization of subgrid cumulus, which has been removed. Other than that, the physics remain the same and the initial conditions are the ones used for the cold start full adjoint sensitivities.

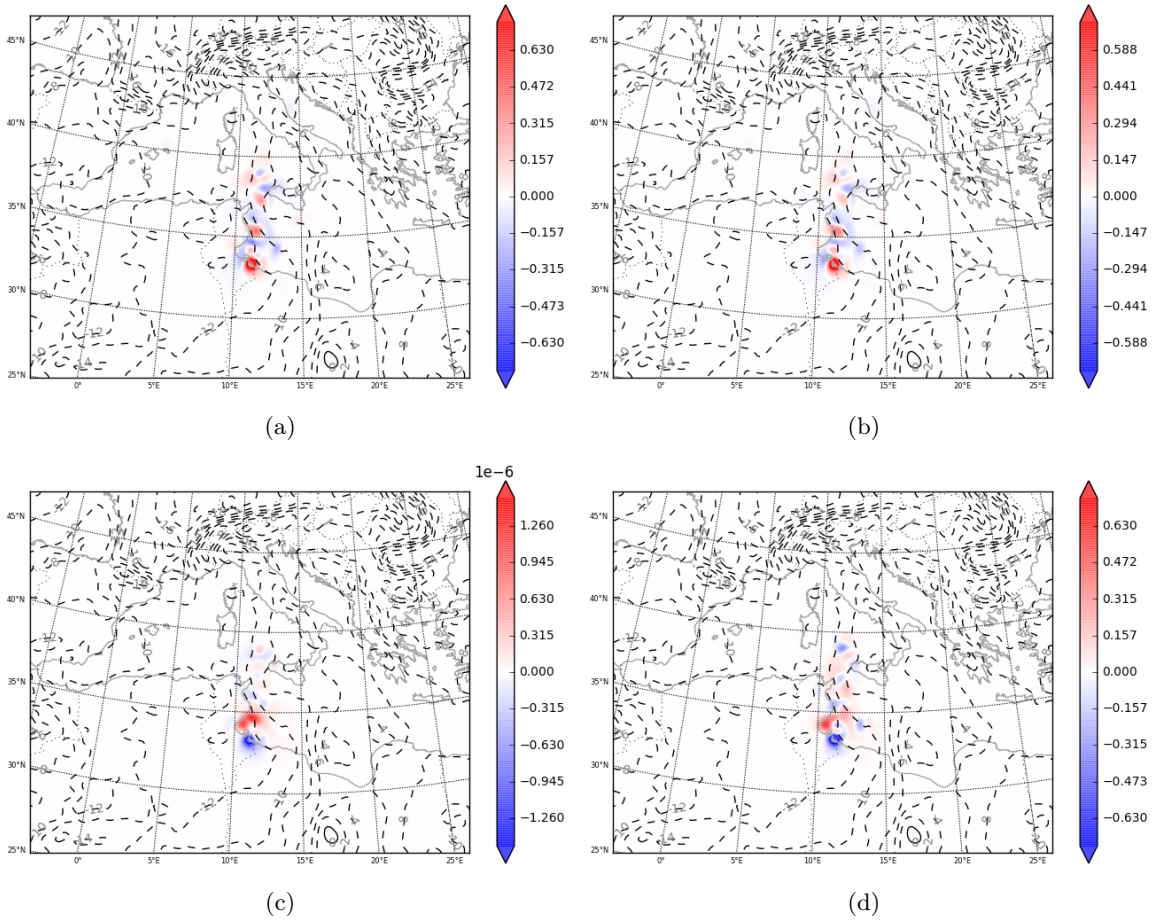

Figure 18: Vertically averaged sensitivity to temperature for a cold start without cumulus parameterization of (a) J_1 (Pa/K), (b) J_2 (Pa/K), (c) J_3 (s^{-1}/K) and (d) J_4 (J/K). Sensitivities are valid for 7 Nov at 00UTC.

The sensitivities to temperature of the selected response functions (figure 18) show the same relation with respect to the sign of sensitivities as the control fields. This confirms the robustness of the adjoint results, which account only for the linearization of the full nonlinear processes. An important point to notice is that deactivating the cumulus parameterization does not particularly change the nature of the sensitivities. These remain highly intense and confined in small areas. In this case, there is a clear dipole of northern warm temperatures and southern cold temperatures favoring the Medicane intensity by the Tunisian coast, right where the cyclone originiated. A closer

look shows also a cold nucleus northern of this warm one, continuing the tripole.This result underlines the role of a warmer core in the preceding cyclonic environment would -under linearized processes- deepen the Medicane at 12UTC. This result is consistent with the tropical characteristics associated with Medicane formation and intensification.

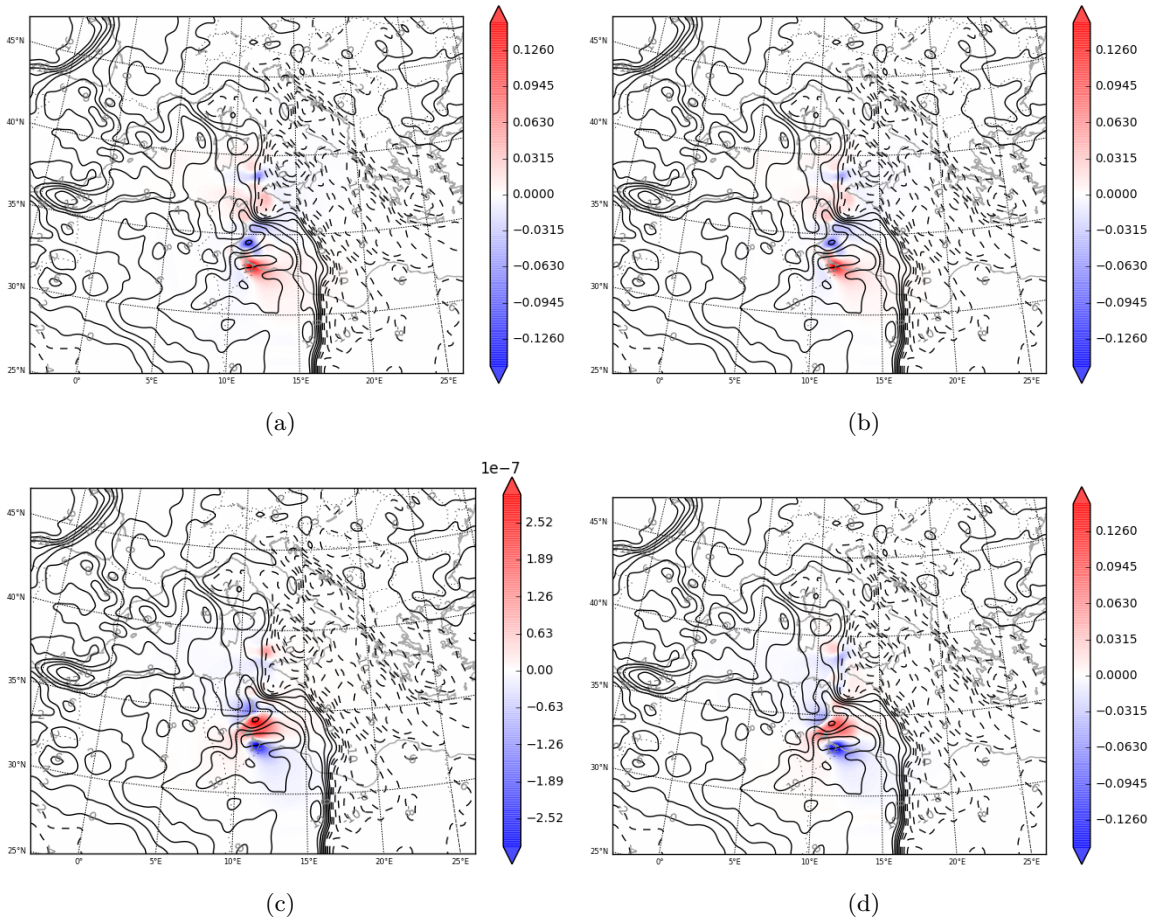

Figure 19: Vertically averaged sensitivity to the u wind component for a cold start without cumulus parameterization of (a) J_1 (Pa/ms^{-1}), (b) J_2 (Pa/ms^{-1}), (c) J_3 (s^{-1}/ms^{-1}) and (d) J_4 (J/ms^{-1}). Sensitivities are valid for 7 Nov at 00UTC.

The sensitivity to the u wind component (figure 19) is similar to the temperature one. In this case, the tripole favoring the cyclone has a south to north structure of westard-eastward-westward direction of u. The top dipole of this tripole corresponds to a generation of cyclonic circulation which would favor the cyclone intensity. The bottom negative sensitivity indicates that a smoother velocity field would have favored the cyclogenesis.

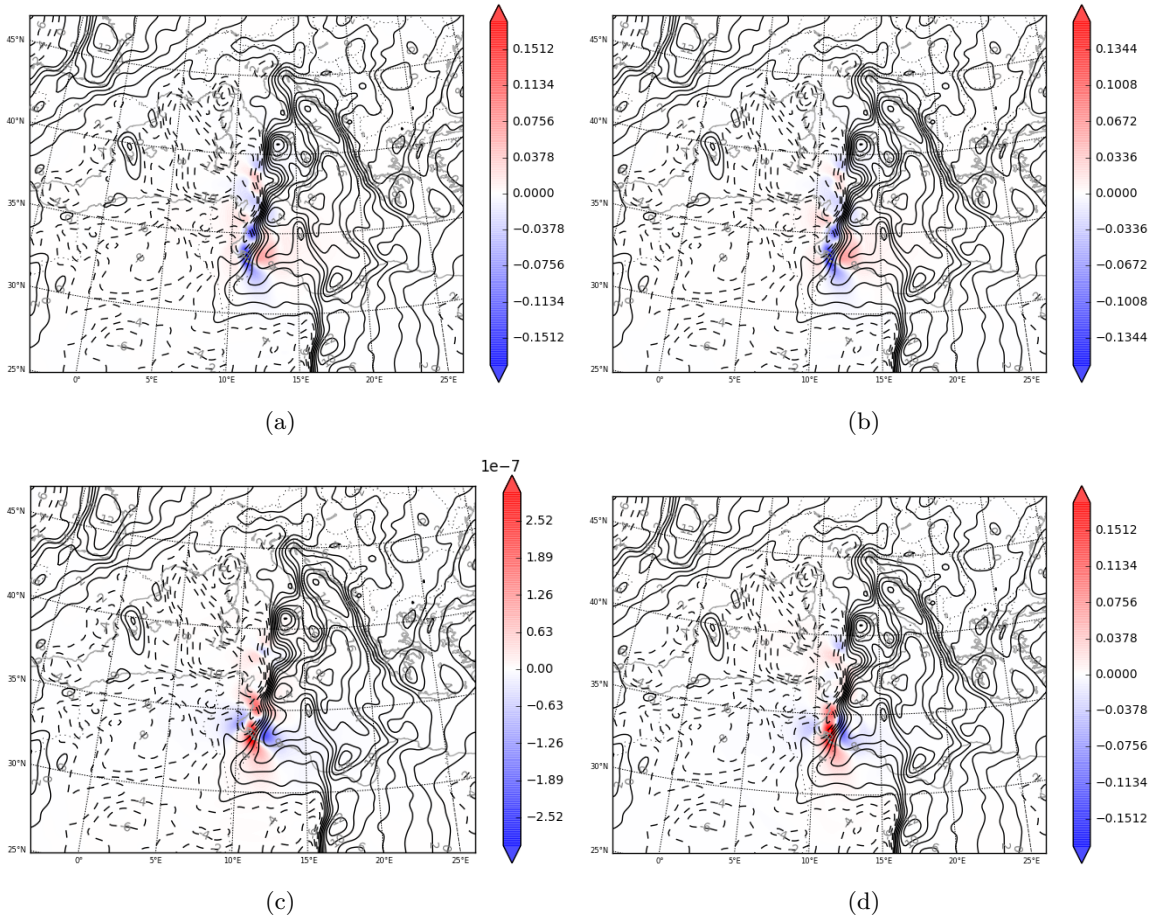

Figure 20: Vertically averaged sensitivity to the v wind component for a cold start without cumulus parameterization of (a) J_1 (Pa/ms^{-1}), (b) J_2 (Pa/ms^{-1}), (c) J_3 (s^{-1}/ms^{-1}) and (d) J_4 (J/ms^{-1}). Sensitivities are valid for 7 Nov at 00UTC.

The case for the sensitivity to the v wind component (figure 20) is not very different from that of the temperature and u, as it displays a west-east tripole of southward-northward-southward velocities favoring the intensity of the cyclone. Furthermore, the central northward velocity nucleus is split in two different positive nuclei, one to the north of the other. The northern positive velocity nucleus combined with the negative westmost negative nucleus are representative that an intensification of the cyclonic circulation displaced to the west of the surface low at 00UTC would favor the formation of the cyclone. However, the remaining intense positive-negative dipole acts exactly opposite to the south of the surface low, and indicates that a reduction of the wind shear and an isolation of this cyclonic circulation would generate a more intense Medicane at 12UTC.

All in all, the information given by these sensitivities without cumulus parameterization has been in agreement with that of the full adjoint sensitivities. Firstly, a warm isolated center at 00UTC would intensify the Medicane at 12UTC. As for the wind fields, both were indicative that an intensified initial cyclonic circulation would also be beneficial to the cyclogenesis.

4.3 Impact of latent heat release on adjoint sensitivities

This simulation has no parameterization of subgrid cumulus, like the previous one. In addition, the release of latent heat from microphysical species is deactivated. Again, the initiator of the simulation is the cold start used for the adjoint complete simulations.

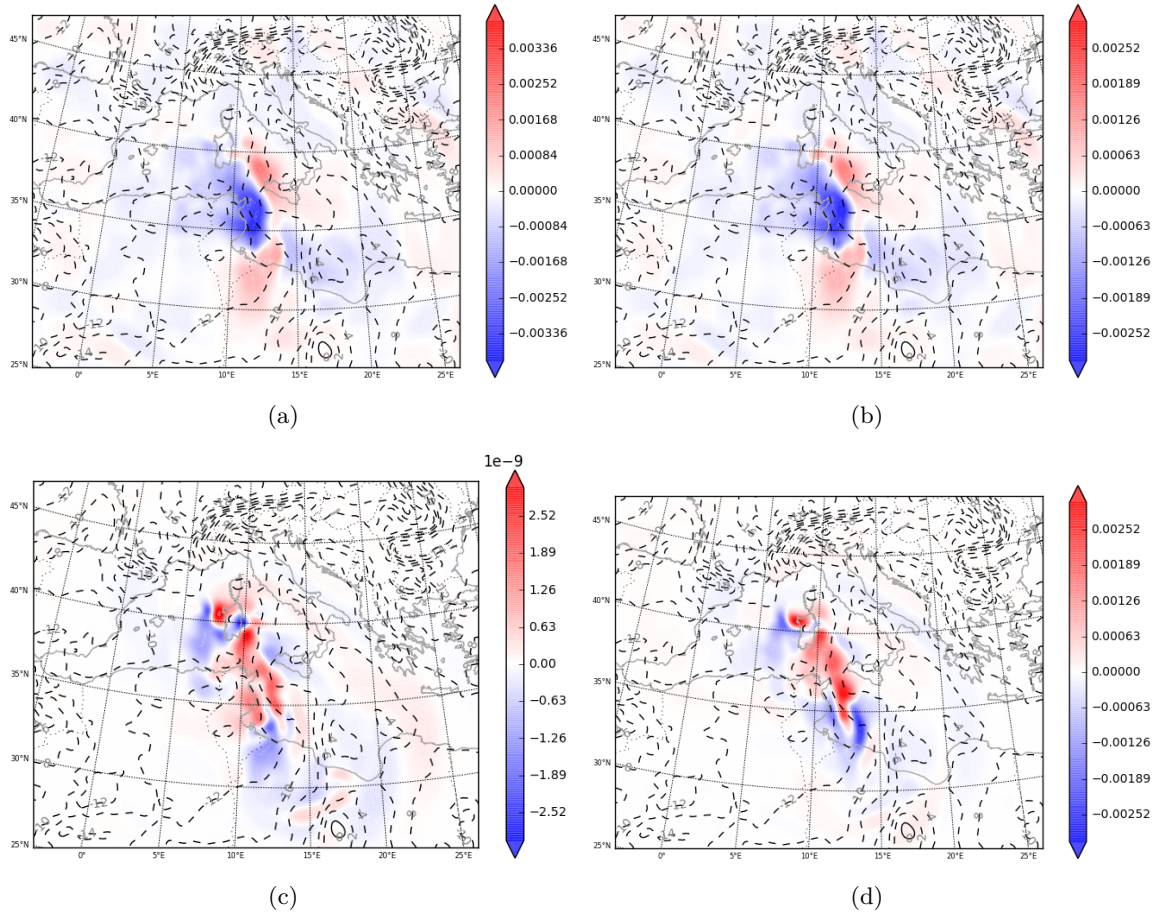

Figure 21: Vertically averaged sensitivity to temperature for a cold start without cumulus parameterization or latent heat release of (a) J_1 (Pa/K), (b) J_2 (Pa/K), (c) J_3 (s^{-1}/K) and (d) J_4 (J/K). Sensitivities are valid for 7 Nov at 00UTC.

When the latent heat release from microphysical species is deactivated, the structure of the sensitivities to temperature (figure 21) is clearly larger and generally of smaller intensity. The sensitivities to temperature are consistent through different response functions in the warm area located over the sea level pressure low at 00UTC that would be favorable to the cyclone formation. These sensitivities fit with the theory that a warm center would favor the formation of a Medicane at 12UTC. However, in this case that warm center is not so isolated and can not be associated to latent heat release as an intensification mechanism for the cyclone. A possible explanation for the positive sensitivity zone is that warmer temperatures would favor evaporation from the sea. Besides, the warmer air can contain larger quantities of water vapor, an intensifying factor for the cyclone.

Another important point to notice is that both pressure response functions are consistent with one another whereas the relative vorticity sensitivities and the weighted total dry energy sensitivi-

ties differ significantly from the pressure ones and are only slightly similar between them. However, a common interpreation to all four response functions has been possible. There seems to be an indication that the previously mentioned agreement between the different response functions was partly due to the most intense structures being related to cumulus formation (with the size of the grid or subgrid) and latent heat release overshadowing the less intense more distinctive characteristics.

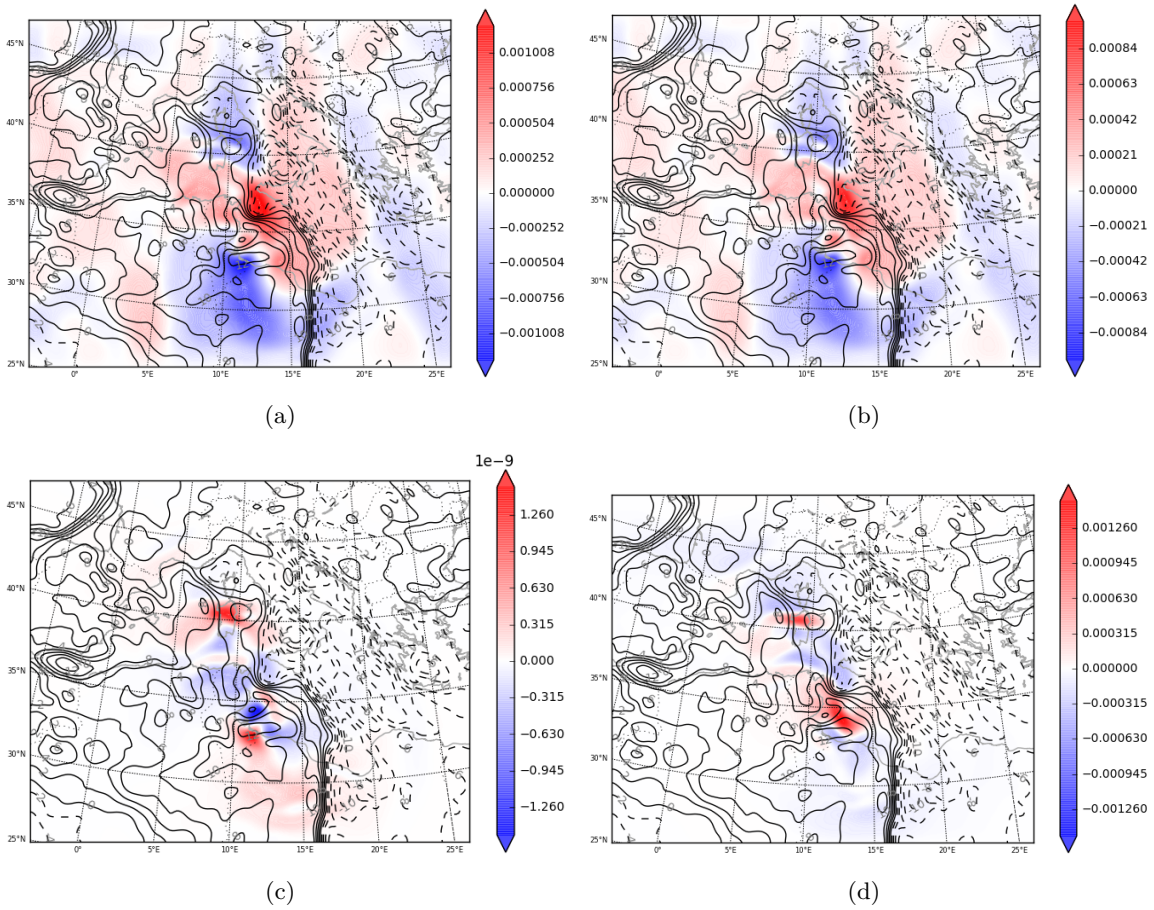

Figure 22: Vertically averaged sensitivity to the u wind component for a cold start without cumulus parameterization or latent heat release of (a) J_1 (Pa/ms^{-1}), (b) J_2 (Pa/ms^{-1}), (c) J_3 (s^{-1}/ms^{-1}) and (d) J_4 (J/ms^{-1}). Sensitivities are valid for 7 Nov at 00UTC.

The sensitivities to the u wind component (figure 22) show even larger differences between the pressure response functions and the other two. However, all sensitivity fields agree on the basic interpretation: a more intense cyclonic circulation over the surface low at 00UTC would help intensify the Medicane at 12UTC. There is also a strong positive nucleus to the east of Corsica in the relative vorticity sensitivities which remains unexplained but could be associated to the presence of a gravity wave that coincidentally arrives to the selected area just in time. It is important to notice that for the pressure response functions there is an intensification of the cyclonic circulation, but it is eclipsed by an overall increase in the eastward velocities.

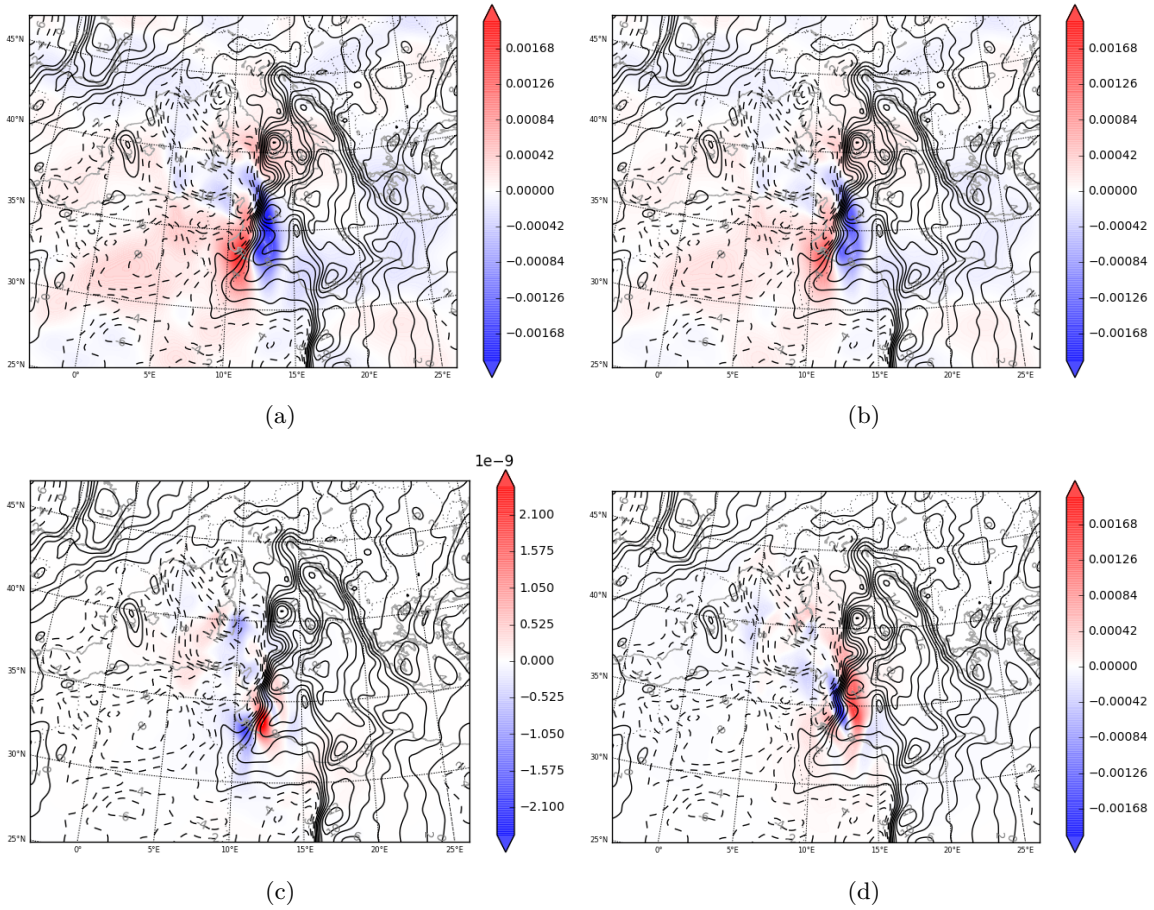

Figure 23: Vertically averaged sensitivity to the v wind component for a cold start without cumulus parameterization or latent heat release of (a) J_1 (Pa/ms^{-1}), (b) J_2 (Pa/ms^{-1}), (c) J_3 (s^{-1}/ms^{-1}) and (d) J_4 (J/ms^{-1}). Sensitivities are valid for 7 Nov at 00UTC.

The sensitivities to the v wind component (figure 23) again show an agreement between the different response functions as all of them show that an intensification of the shear in the south-north direction over the surface low at 00UTC would favor the formation of the Medicane at 12UTC.

The overall structure of the sensitivities is the same for J_1 and J_2 but these differ from the shape of the sensitivities of J_3 and J_4, as already occured for the sensitivities to temperature and u. This agreement between the general behaviour of the different sensitivity fields without latent heat release or cumulus parameterization seems to be an indicator of the aforementioned overshadowing. The sensitivities where latent heat release was present showed more localized but more intense structures. This confirms the suspicion that intense structures associated to the latent heat release and which were common to the sensitivities of all response functions eclipsed the differences between them.

To sum up the sensitivities without latent heat release, a summary of the obtained results can be made. First, the location of the cyclone at its initial stage over a warm area would be favorable to its genesis. Furthermore, the sensitivities to the velocity fields indicate that a more intense cyclonic circulatio at 00UTC would have generated a more intense Medicane at 12UTC. These interpretations are (again) consistent with those of the full adjoint model.

5 Linearity verification

As already stated multiple times in this document, linearity is one of the most limiting factors of the adjoint model. In this context, a verification of the linearity of the model can help understand where this limitation of the adjoint lies.

5.1 WRFPLUS linearity check

As a first linearity check of the evolution of perturbations for this case, the feature included in the standard distribution of WRFPLUS is used.

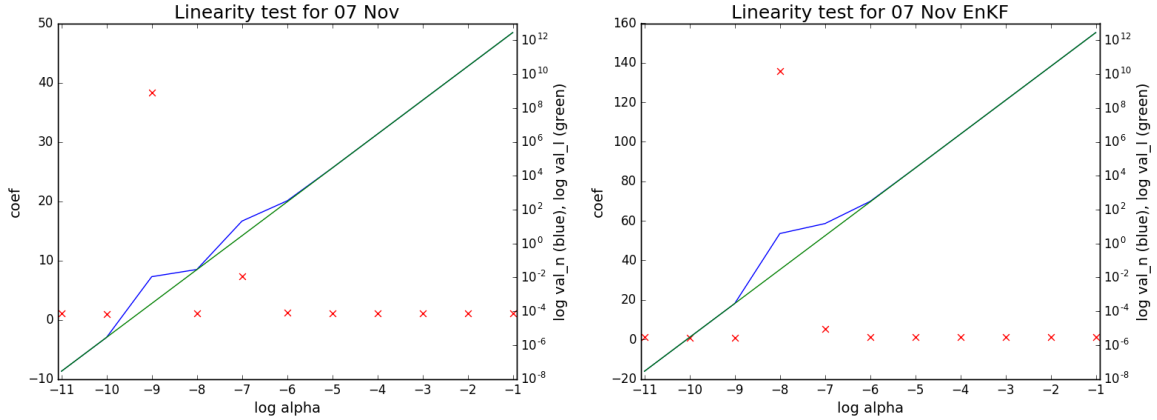

(a) (b)

Figure 24: Model linearity check of November 7th for (a) cold start and (b) warm start. The green and blue line represent the linear and non-linear value of the perturbed evolution. Red crosses represent the quotient of the blue line and the green line. Values of one represent perfect agreement between non-linear and linear evolution of perturbation

The linearity check of the model can be seen in figure 24 for both the cold and the warm start runs. The important point to extract is that the model is highly non-linear and some amplitudes generate very signifivative differences. These amplitudes are not necessarily the biggest ones, which indicates that probably the non-linearities are often present as bifurcation points (e.g. on-off switches for convection), and not only in the form of general non-linearities.

5.2 Verification with perturbation

A more specific linearity test to the case study can be done by quantifying the changes in the evolution of differently scaled perturbations of interest to the initial conditions. In essence, this linearity check is focused towards the evolution of perturbations that affect a specific response function. In particular, the perturbation is built by rescaling the adjoint sensitivity fields to a specified range of amplitudes. The choice of reference perturbation will be the output of the adjoint model itself for pressure sensitivity to temperature (the sensitivity field) scaled to its maximum, so that the field reaches the maximum value of 1. Since the whole adjoint process relies on the linearity of the model, this perturbation will then be scaled to different amplitudes in order to check for this linearity. A non-linear WRF simulation is run for each set of perturbed initial conditions and

the response function is calculated. Then, the control response function is substracted from this perturbed response function. The relation of this difference with respect to amplitude is seen in figure 25. This representations would be expected to form a straight line for a perfectly linear evolution, so the closer these points are to a line, the more linear the evolution is.

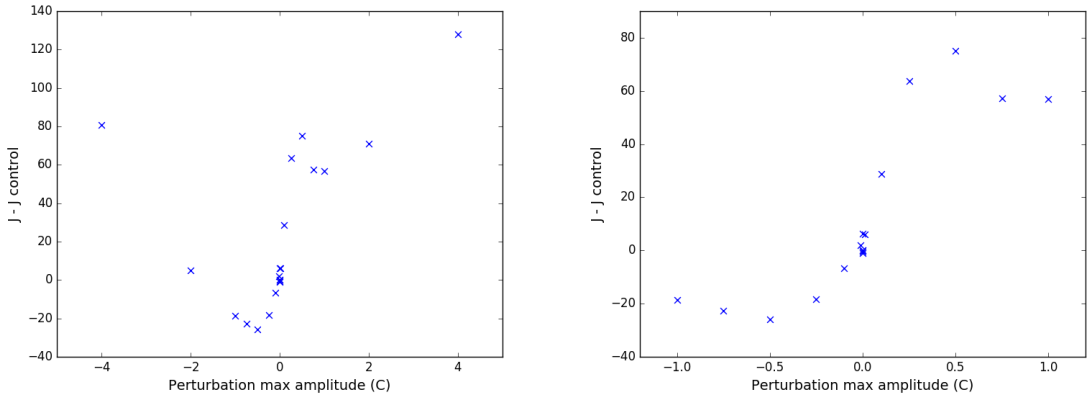

(a) (b)

Figure 25: Verification of the linearity of the simulation with the amplitude of perturbation (a) zoomed into the linear zone (b)

In this case, the response function taken is simply the pressure prism (J_1) and it is important to notice that the phenomenon in study is an extreme pressure minimum. This means that the conditions to deepen it further are less likely than the range of perturbations that produce cyclolysis. Therefore, the most frequent expected responses for J_1 are those that fill the pressure field. The fact that with some amplitudes of the negative perturbations J_1 decreases and the linear shape taken by the small perturbation areas leads to think that linearity can be assumed in that interval and that the adjoint model provides sensible information for at least a certain range of perturbation amplitudes.

5.3 Impact of latent heat release on linearity

With the visualization of regular moist sensitivities, sensitivities without cumulus parameterization and sensitivities without cumulus parameterization or latent heat release, a clear tendency has arised. Both of the sensitivities allowing latent heat release show more localized but more intense structures than the sensitivities with latent heat release deactivated. This is clear evidence that the processes involving latent heat release form microphysical species are dominant in the development of this cyclone. Therefore, when it is removed, other processes previously eclipsed by this latent heat release can arise and display their contribution.

It has been seen that simulations without cumulus parameterization and regular moist sensitivities do not differ significantly in their general structure. However, there is a representative difference between the moist sensitivities and the sensitivities without latent heat release. This makes a comparison of their linearity a very interesting tool to undertand how they behave.

Again, the perturbation has been selected as the same sensitivity field normalized to its maximum value (in absolute value) and then scaled by a parameter α. As this has been done for both

initial conditions, each of them has been perturbed with its correponding sensitivity field.

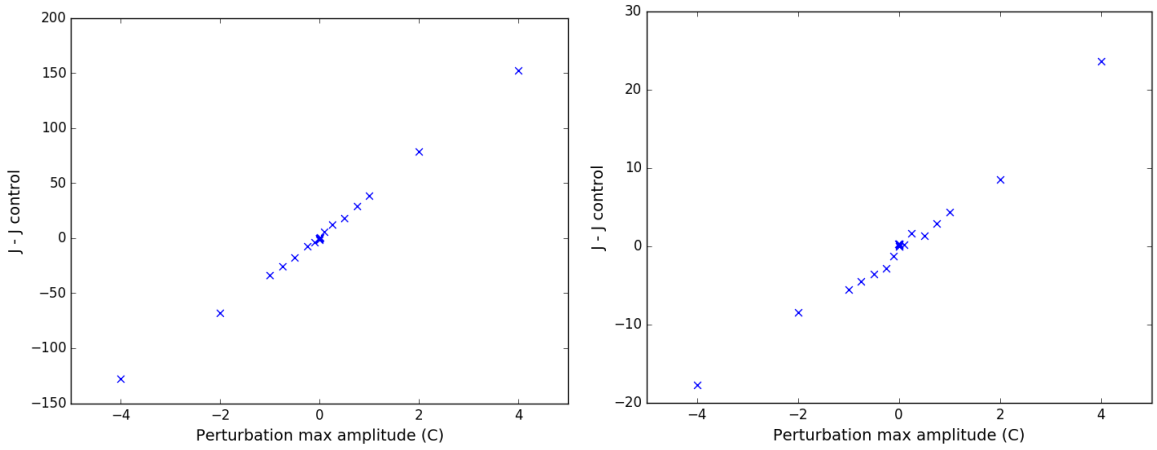

(a) (b)

Figure 26: Linearity checks without cumulus parameterization or latent heat release for (a) cold start and (b) warm start

These linearity checks (figure 26) show that there is a clear linear tendency for the response function variation with respect to perturbation. This tendency is much more linear for the cold start fields. Also, for both types of initial conditions the positive perturbations have stronger effects than the negative ones. This difference in the two initial conditions and the uneven effect of the different sign perturbations would not be expected from perfect linearity, but this simulation still contains non-linear effects since only latent heat release from microphysical species has been deactivated and other generators of non-linearity are present. As reinforcement of the linearity results obtained by the perturbation, the WRFPLUS linearity check is also run for the case without parameterized cumulus of latent heat release from microphysical species.

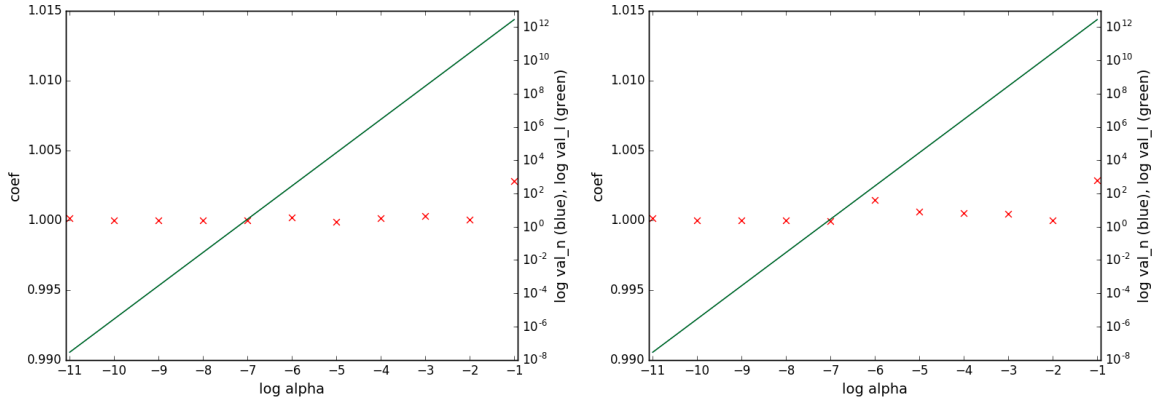

(a) (b)

Figure 27: Model linearity check of November 7th without cumulus parameterization or latent heat release for (a) cold start and (b) warm start. The green and blue line represent the linear and non-linear value of the perturbed evolution. Red crosses represent the quotient of the blue line and the green line. Values of one represent perfect agreement between non-linear and linear evolution of perturbation

The model linearity check for the case without latent heat release shows the almost perfectly linear behaviour of the simulation. All of the values are very close to one, indicative of the agreement between the non-linear and the tangent linear simulations of the perturbation.

6 Summary and conclusions

In the science of prediction, the illusion to get a comprehensive control on the aspects and processes that influence the most threatening features of a forecast is highly appealing. This information (i.e. sensitivity) opens a powerful range of tools, from targeting of extra observations to ensemble generation methods, to progress towards reliable and accurate weather predictions. This work explores various methods to compute forecast sensitivities of a Medicane detected near the coasts of Sicily during 7 November 2014. The flagship in numerical sensitivity calculations is the adjoint model, which is defined within a context tangent linear to the standard non-linear evolution of the simulated atmosphere. This somewhat severe limitation intrinsic to the adjoint requires for a very careful treatment of its results. Detailed interpretation and verification of adjoint sensitivity fields are necessary before they can be transferred to any practical application. This interpretation and verification processes are multifaceted by nature, and a large amount of the work done in this study refers to these processes of quality check of adjoint sensitivity fields.

We perform two standard linearity tests on the evolution of perturbations in the full nonlinear model. These tests reveal that only a small range of perturbations evolve linearly in the control run for this particular cyclogenetic case. With the aim of determining the impact of important nonlinear processes in the deviation of perturbations from linearity, sensitivity experiments with no parameterized convection or latent heat release from microphysical species are performed. These experiments reveal that the cumulus parameterization does not affect significantly the general structure of the sensitivity field. However, the absence of latent heat release from the microphysical species lead to very different results, generating larger areas of smaller sensitivity instead of intense localized ones.

Sensitivity fields have shown an agreement with previous knowledge regarding Medicanes. Almost all sensitivities computed in this study agreed in that a particularly warm center with respect to the surroundings is favorable to the genesis of an intense Medicane. This agreement extended to the sensitivities to the wind field. Again, the vast majority of sensitivities agreed that an increase of the cyclonic circulation in the initial conditions would have favored the formation of a more intense cyclone. However, there were cases where sensitivities indicated that a shift in this circulation in some direction would have been more favorable. Either way, the original presence of cyclonic circulation has been a persistent indicator of a more intense forecast Medicane 12 hours ahead.

A few different conclusions can be extracted from this work. The first is the relevance of latent heat release in the formation and intensification of the cyclone. This result is consistent with previous knowledge about Medicanes, which as tropical-like cyclones use the latent heat the droplets release when they condensate as an intensification mechanism. The other is the importance of a warm area for cyclone formation even when the latent heat release is turned off. This is representative of the fact that higher temperatures favor evaporation from the sea and also that warmer air can contain more water than colder air, which will later form clouds even though its release of latent heat is turned off. Furthermore, cyclonic circulation is a consistent factor favorable to the genesis of the Medicane.

Finally, another important point to mention is linearity, as it is probably the most limiting factor of the adjoint model. The full sensitivities have been proven to be quasi-linear for a limited range of perturbations. However, a deactivation of the latent heat release has made this zone of linear amplitudes expand, at least, to the range of amplitudes covered here. Also, this linearity has been proven to be clearer for a cold start than for a warm start, which shows smoother structures

since it is a direct downscaling of a global model, making the presence of microphysical species practically null.

Elegant cause-effect information about the genesis and evolution of a Medicane was derived in this work. Sensitivity information is a powerful tool that requires careful expert treatment. Future research will abound on new methods to describe sensitivity information and techniques to reliably put them to the use of improved high impact weather forecasts.

Bibliography

Ancell, B. and G. J. Hakim, 2007: Comparing Adjoint- and Ensemble-Sensitivity Analysis with Applications to Observation Targeting. *Monthly Weather Review*, **135** (12), 4117–4134. doi:10.1175/2007MWR1904.1.

Carrió, D., V. Homar, A. Jansà, R. Romero, and M. A. Picornell, 2017: Tropicalization Process of the 7 November 2014 Mediterranean Cyclone: Numerical Sensitivity Study. *Atmospheric Research*.

Cavicchia, L., H. von Storch, and S. Gualdi, 2014a: A long-term climatology of medicanes. *Climate Dynamics*, **43** (5-6), 1183–1195. ISSN 14320894. doi:10.1007/s00382-013-1893-7.

Cavicchia, L., H. Von Storch, and S. Gualdi, 2014b: Mediterranean tropical-like cyclones in present and future climate. *Journal of Climate*, **27** (19), 7493–7501. ISSN 08948755. doi:10.1175/JCLI-D-14-00339.1.

Charney, J. G., 1951: Dynamic forecasting by numerical process. In *Compendium of meteorology*, pages 470–482. Springer.

Cioni, G., P. Malguzzi, and A. Buzzi, 2016: Thermal structure and dynamical precursor of a Mediterranean tropical-like cyclone. *Quarterly Journal of the Royal Meteorological Society*, **142** (697), 1757–1766. ISSN 00359009. doi:10.1002/qj.2773.

Doerenbecher, A. and T. Bergot, 2001: Sensitivity to observations applied to FASTEX cases. *Nonlinear Processes in Geophysics*, **8** (6), 467–481. ISSN 10235809. doi:10.5194/npg-8-467-2001.

Drobinski, P., V. Ducrocq, P. Alpert, E. Anagnostou, K. Béranger, M. Borga, I. Braud, A. Chanzy, S. Davolio, G. Delrieu, C. Estournel, N. Filali Boubrahmi, J. Font, V. Grubišić, S. Gualdi, V. Homar, B. Ivančan-Picek, C. Kottmeier, V. Kotroni, K. Lagouvardos, P. Lionello, M. C. Llasat, W. Ludwig, C. Lutoff, A. Mariotti, E. Richard, R. Romero, R. Rotunno, O. Roussot, I. Ruin, S. Somot, I. Taupier-Letage, J. Tintor, R. Uijlenhoet, and H. Wernli, 2014: HYMEX: A 10-year multidisciplinary program on the mediterranean water cycle. *Bulletin of the American Meteorological Society*, **95** (7), 1063–1082. ISSN 00030007. doi:10.1175/BAMS-D-12-00242.1.

Ehrendorfer, M., 2000: The Total Energy Norm in a Quasigeostrophic Model. *Journal of the Atmospheric Sciences*, **57** (20), 3443–3451. ISSN 0022-4928. doi:10.1175/1520-0469(2000)057¡3443:NACTEN¿2.0.CO;2.

Errico, R. M., 1997: What Is an Adjoint Model? *Bulletin of the American Meteorological Society*, **78** (11), 2577–2591. ISSN 00030007. doi:10.1175/1520-0477(1997)078¡2577:WIAAM¿2.0.CO;2.

Errico, R. M., 2007: Interpretations of an adjoint-derived observational impact measure. *Tellus, Series A: Dynamic Meteorology and Oceanography*, **59** (2), 273–276. ISSN 02806495. doi:10.1111/j.1600-0870.2006.00217.x.

Fisher, M., J. Nocedal, Y. Trémolet, and S. J. Wright, 2009: Data assimilation in weather forecasting: A case study in PDE-constrained optimization. *Optimization and Engineering*, **10** (3), 409–426. ISSN 13894420. doi:10.1007/s11081-008-9051-5.

Fowler, A., 1963: Data Assimilation tutorial on the Kalman filter. *University of Reading*.

Garcies, L. and V. Homar, 2014: Are current sensitivity products sufficiently informative in targeting campaigns? A DTS-MEDEX-2009 case study. *Quarterly Journal of the Royal Meteorological Society*, **140** (679), 525–538. ISSN 1477870X. doi:10.1002/qj.2148.

Hart, R. E., 2003: A Cyclone Phase Space Derived from Thermal Wind and Thermal Asymmetry. *Monthly Weather Review*, **131** (4), 585–616. ISSN 0027-0644. doi:10.1175/1520-0493(2003)131¡0585:ACPSDF¿2.0.CO;2.

Holton, J. R., 2004: *An Introduction to Dynamical Meteorology*. Elsevier Academic Press, Burlington, MA, Fourth edition.

Homar, V., R. Romero, D. J. Stensrud, C. Ramis, and S. Alonso, 2003: Numerical diagnosis of a small, quasi-tropical cyclone over the western Mediterranean: Dynamical vs. boundary factors. *Quarterly Journal of the Royal Meteorological Society*, **129** (590 PART A), 1469–1490. ISSN 00359009. doi:10.1256/qj.01.91.

Homar, V. and D. J. Stensrud, 2004: Sensitivities of an intense Mediterranean cyclone: Analysis and validation. *Quarterly Journal of the Royal Meteorological Society*, **130** (602 PART A), 2519–2540. ISSN 00359009. doi:10.1256/qj.03.85.

Homar, V. and D. J. Stensrud, 2008: Subjective versus objective sensitivity estimates: Application to a North African cyclogenesis. *Tellus, Series A: Dynamic Meteorology and Oceanography*, **60** (5), 1064–1078. ISSN 02806495. doi:10.1111/j.1600-0870.2008.00353.x.

Jansa, A., P. Alpert, P. Arbogast, A. Buzzi, B. Ivancan-Picek, V. Kotroni, M. C. Llasat, C. Ramis, E. Richard, R. Romero, and A. Speranza, 2014: MEDEX: A general overview. *Natural Hazards and Earth System Sciences*, **14** (8), 1965–1984. ISSN 16849981. doi:10.5194/nhess-14-1965-2014.

Jung, B.-J., H. M. Kim, T. Auligné, X. Zhang, X. Zhang, and X.-Y. Huang, 2013: Adjoint-Derived Observation Impact Using WRF in the Western North Pacific. *Monthly Weather Review*, **141** (11), 4080–4097. ISSN 0027-0644. doi:10.1175/MWR-D-12-00197.1.

Kalnay, E., 2003: *Atmospheric modeling, data assimilation and predictability*. Cambridge University Press.

Kim, H. M., M. C. Morgan, and R. E. Morss, 2004: Evolution of Analysis Error and Adjoint-Based Sensitivities: Implications for Adaptive Observations. *Journal of the Atmospheric Sciences*, **61**, 795–812. ISSN 0022-4928. doi:10.1175/1520-0469(2004)061¡0795:EOAEAA¿2.0.CO;2.

Leutbecher, M., 2003: Adaptive observations, the Hessian metric and singular vectors. *Proc. ECMWF Seminar on Recent developments in data assimilation for atmosphere and ocean, Reading, UK*, (1997), 8–12.

Lorenz, E. N., 1963: Deterministic nonperiodic flow. *Journal of the atmospheric sciences*, **20** (2), 130–141.

Majumdar, S. J., 2016: A review of targeted observations. *Bulletin of the American Meteorological Society*, **97** (12), 2287–2303. ISSN 00030007. doi:10.1175/BAMS-D-14-00259.1.

Mandel, J., 2009: A Brief Tutorial on the Ensemble Kalman Filter. (February 2007), 1–7.

Mazza, E., U. Ulbrich, and R. Klein, 2017: The Tropical Transition of the October 1996 Medicane in the Western Mediterranean Sea: A Warm Seclusion Event. *Monthly Weather Review*, **145** (7), 2575–2595. ISSN 0027-0644. doi:10.1175/MWR-D-16-0474.1.

Michaelides, S., T. Karacostas, J. L. Sánchez, A. Retalis, I. Pytharoulis, V. Homar, R. Romero, P. Zanis, C. Giannakopoulos, J. Bühl, A. Ansmann, A. Merino, P. Melcón, K. Lagouvardos, V. Kotroni, A. Bruggeman, J. I. López-Moreno, C. Berthet, E. Katragkou, F. Tymvios, D. G.

Hadjimitsis, R.-E. Mamouri, and A. Nisantzi, 2017: Reviews and perspectives of high impact atmospheric processes in the Mediterranean. *Atmospheric Research*. ISSN 0169-8095. doi: https://doi.org/10.1016/j.atmosres.2017.11.022.

Miglietta, M. M., S. Laviola, A. Malvaldi, D. Conte, V. Levizzani, and C. Price, 2013: Analysis of tropical-like cyclones over the Mediterranean Sea through a combined modeling and satellite approach. *Geophysical Research Letters*, **40** (10), 2400–2405. ISSN 00948276. doi:10.1002/grl.50432.

Picornell, M., A. Jansà, A. Genovès, and J. Campins, 2001: Automated database of mesocyclones from the HIRLAM(INM)-0.5 analyses in the western Mediterranean. *International Journal of Climatology*, **21** (3), 335–354. ISSN 08998418. doi:10.1002/joc.621.

Picornell, M. A., J. Campins, and A. Jansà, 2014: Detection and thermal description of medicanes from numerical simulation. *Natural Hazards and Earth System Sciences*, **14** (5), 1059–1070. ISSN 16849981. doi:10.5194/nhess-14-1059-2014.

Romero, R. and K. Emanuel, 2017: Climate change and hurricane-like extratropical cyclones: Projections for North-Atlantic polar lows and medicanes based on CMIP5 models. *Journal of Climate*, **30**, 279–299.

Snyder, C., 1995: Summary of an Informal Workshop on Adaptive Observations and FASTEX. pages 2937–2946.

Thorpe, A., 1985: Predictability and Targeted Observations Theory of Predicting the Location of Sensitive Regions. pages 307–320.

Tous, M. and R. Romero, 2013: Meteorological environments associated with medicane development. *International Journal of Climatology*, **33** (1), 1–14. ISSN 08998418. doi:10.1002/joc.3428.

Vukićević, T. and R. M. Errico, 1993: Linearization and adjoint of parameterized moist diabatic processes. *Tellus A*, **45** (5), 493–510. ISSN 16000870. doi:10.1034/j.1600-0870.1993.0012.x.

Wheatley, D. M. and D. J. Stensrud, 2010: The impact of assimilating surface pressure observations on severe weather events in a WRF mesoscale ensemble system. *Monthly Weather Review*, **138** (5), 1673–1694. ISSN 0027-0644. doi:10.1175/2009MWR3042.1.

Zhang, X., X. Y. Huang, and N. Pan, 2013: Development of the upgraded tangent linear and adjoint of the weather research and forecasting (WRF) model. *Journal of Atmospheric and Oceanic Technology*, **30** (6), 1180–1188. ISSN 07390572. doi:10.1175/JTECH-D-12-00213.1.

Zhong, K., P. Dong, S. Zhao, Q. Cai, and W. Lan, 2007: Adjoint-based sensitivity analysis of a mesoscale low on the mei-yu Front and its implications for adaptive observation. *Advances in Atmospheric Sciences*, **24** (3), 435–448. ISSN 02561530. doi:10.1007/s00376-007-0435-9.

Zou, X., F. Vandenberghe, M. Pondeca, and Y.-H. Kuo, 1997: Introduction to adjoint techniques and the MM5 adjoint modeling system. *NCAR Technical ...*, page 101.

Agraïments

Quan vaig saber que el TFM podia incloure agraïments va ser una alegria molt gran, perquè aquest treball no hauria estat possible sense l'ajuda de moltes persones. Algunes d'aquestes persones han oferit la seva inestimable ajuda en un àmbit personal i d'altres, a més, hi han afegit una aportació científica i una gran ajuda en moments crítics pels resultats finals d'aquest treball.

En primer lloc, vull donar les gràcies a Víctor Homar per la seva paciència, comprensió i ajuda constant i les grans oportunitats que m'ha donat. També vull agrair-li la seva gran disponibilitat sempre que hi ha hagut moments difícils en l'avanç d'aquesta feina i sempre que l'he necessitat en un àmbit personal. I perquè dóna molt de gust fer feina amb algú que es preocupa i que realment s'implica com a persona.

També vull agrair a Diego Carrió la seva ajuda i la seva paciència, sempre que ho he necessitat m'ha donat una mà desinteressadament. Quan he necessitat algú que aconseguís desembossar-me, he pogut recórrer a ell i sempre m'ha ajudat de la millor manera que ha pogut.

Vull agrair en general al grup de meteo la seva acollida, perquè tot i haver-hi entrat a formar part molt recentment, mai he tengut la sensació de ser una nova incorporació. Vull agrair especialment a Romu Romero (i també un altre cop a Víctor Homar) per donar-me l'oportunitat d'anar al meu primer congrés a Viena, una gran experiència que amb la seva presència varen fer que fos encara millor.

Dins el grup de meteo, vull fer també una menció especial als membres del laboratori. Na Maria, en Jordi i na Maria del Mar han estat tres grans descobriments d'aquest any a la vegada que tres suports en el dia a dia, i ha estat un gust poder fer feina al seu costat durant aquests mesos. Costa d'imaginar un millor IT team.

Per últim però no menys important, vull agrair a les persones que fan que en el meu dia a dia a la universitat em senti com a casa. En primer lloc, vull donar les gràcies a en Toni perquè vàrem començar el grau i vàrem fer-nos un equip i seguim fent un gran equip cinc anys després, i perquè ha estat un gust fer tot aquest camí junts. També vull agrair a en Dani per haver-me donat tants moments de rialles, així com suport quan l'he necessitat i ajuda i consell quan ha fet falta. Vull donar les gràcies a n'Albert i a n'Adel, perquè sempre que els veig m'alegren el dia i perquè m'han donat un suport impagable en els moments més durs tot i no poder passar tantes hores junts com ens agradaria. Tots ells m'han fet sentir recolzada i en família en tot moment, el qual no crec que els hi pugui agrair mai prou.

Per acabar, vull agrair a la meva família el seu suport en tot moment, per haver-me aguantat quan estava de mal humor perquè les coses no sortien, per no enfadar-se quan he arribat molt tard a casa perquè no sortia de la universitat fins que no arreglés el problema de torn, per haver-me obligat a desconnectar quan era necessari i per sempre haver tengut un somriure quan feia falta. Vull donar les gràcies al meu pare i el meu germà per no haver deixat de ser un equip en cap moment i per haver-nos mantingut com una pinya sempre.

I vull donar les gràcies a la meva mare, per haver estat sempre el meu major suport i la persona a qui podia contar-li qualsevol cosa. Perquè sempre ha pensat més en jo que en ella mateixa, cosa que ha fet que aquest treball hagi estat possible. I perquè l'enyor molt, però encara així em segueix donant força. Tant de bo estiguis orgullosa.